
MASTER THESIS

COMSOL MODEL OF THE MEASUREMENT SETUP OF IN-EAR HEADPHONES

conducted at the
Signal Processing and Speech Communications Laboratory
Graz University of Technology, Austria

in co-operation with
USound GmbH
Vienna, Austria

by
Georg Klein, BSc. BSc. BMus.

Supervisor:
Dipl.-Ing. Dr.techn. Werner Weselak

Graz, September 14, 2021

Abstract

In this work, a finite element model of an in-ear headphone in a standardized ear simulator (IEC 60318-4) is presented. The Comsol Multiphysics 5.6 software is used for simulation. The model replicates the typical measurement setup used to evaluate in-ear headphones and serves as the basis for a headphone development application. The headphone geometry must therefore be easily interchangeable. Submodels for a venting hole and an acoustic fleece are included considering this requirement. Wave propagation in the air volume between the loudspeaker membrane in the headphone and the microphone membrane in the ear simulator is modelled. The ear simulator is replaced by its input impedance and transfer function. The results of the simplified impedance model match perfectly with the full model.

The model's input is the membrane velocity of the loudspeaker. It is determined by measurements on a laser Doppler vibrometer. The model is validated by measurements in the ear simulator with different insertion depths of the headphone, different venting holes and different acoustic fleeces. The comparison of simulation and measurement mostly confirms the model. For the thinnest venting hole, a correction factor is established. Further investigations with other hole sizes are necessary. The submodel for the acoustic fleece could be improved by determining further material parameters.

Zusammenfassung

In dieser Arbeit wird ein Finite-Elemente-Modell eines In-Ear-Kopfhörers in einem genormten Ohrsimulator (IEC 60318-4) vorgestellt. Zur Simulation wird die Software Comsol Multiphysics 5.6 verwendet. Das Modell bildet den typischen Messaufbau zur Beurteilung von In-Ear-Kopfhörern nach und dient als Grundlage für eine Kopfhörer-Entwicklungsanwendung. Die Kopfhörergeometrie muss deshalb leicht austauschbar sein. Untermodelle für ein Belüftungsloch und ein akustisches Vlies werden unter Berücksichtigung dieser Vorgabe eingebunden. Simuliert wird die Wellenausbreitung im Luftvolumen zwischen der Lautsprechermembran im Kopfhörer und der Mikrofonmembran im Ohrsimulator. Der Ohrsimulator wird dabei durch seine Eingangsimpedanz und Übertragungsfunktion ersetzt. Die Ergebnisse des vereinfachten Impedanzmodells stimmen perfekt mit dem vollständigen Modell überein.

Die Eingangsgröße des Modells ist die Membranschnelle des Lautsprechers. Diese wird durch Messungen am Laser-Doppler-Vibrometer bestimmt. Validiert wird das Modell anhand von Messungen im Ohrsimulator mit verschiedenen Einstecktiefen des Kopfhörers, verschiedenen Belüftungslöchern und verschiedenen Akustik-Vliesen. Der Abgleich von Simulation und Messung bestätigt das Modell weitgehend. Für das dünnste Belüftungsloch wird ein Korrekturfaktor ermittelt. Weitere Untersuchungen mit anderen Lochgrößen sind notwendig. Das Untermodell für das Akustikvlies könnte durch die Bestimmung weiterer Materialparameter verbessert werden.

Statutory Declaration

I declare that I have authored this thesis independently, that I have not used other than the declared sources/resources, and that I have explicitly marked all material which has been quoted either literally or by content from the used sources.

date

(signature)

Contents

1	Introduction	9
1.1	Motivation	9
1.2	Problem Description	9
1.3	Approach	10
2	Comsol Simulation	11
2.1	Comsol Multiphysics	11
2.2	Headphone Model	15
2.3	Adapter Model	19
2.3.1	venting hole	21
2.3.2	acoustic fleece	29
2.4	Ear Simulator Model	34
2.4.1	input impedance and transfer function	35
2.4.2	impedance model vs. full model	36
3	Measurements and Validation	41
3.1	Membrane Velocity	41
3.2	SPL inside the Ear Simulator	44
3.2.1	equipment and setup	44
3.2.2	variation of insertion depth	46
3.2.3	variation of venting	49
3.2.4	variation of acoustic fleece	56
4	Conclusion	61
4.1	Summary	61
4.2	Limitations and Future Work	62

1

Introduction

1.1 Motivation

The company USound GmbH is specialized on the development of loudspeakers using MEMS (micro-electro-mechanical system) technology. These speakers can be used in various devices. A current topic is the design and optimization of in-ear headphones with the Achelous UT-P2018 loudspeaker. The speaker is shown in figure 1.1, its data sheet can be found in [1].

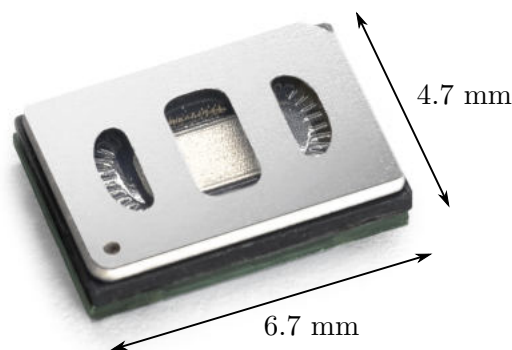


Figure 1.1: MEMS loudspeaker type Achelous from USound with sizes [1]

To reduce the need of expensive and time consuming prototyping for the headphone development, a finite element model is required. It is important that the resulting model can be used and adjusted easily by non simulation experts, e.g. the field application engineers or the customers, to evaluate the performance of the loudspeaker in a given headphone geometry. Therefore, the goal is to create a headphone development application with a user friendly interface, based on a finite element simulation of the headphone. This thesis presents the numerical model and its validation. The final user interface is developed outside the scope of this work.

1.2 Problem Description

The performance of an in-ear headphone driven by the USound Achelous speaker (see figure 1.1) should be evaluated with a finite element model. In measurements, in-ear headphones are analysed with a standardized ear simulator to represent the acoustic behaviour inside of an average human ear. The model should be consistent with this measurement setup. It is therefore required to model the acoustic domain from the speaker's membrane to the microphone inside the ear simulator.

The model's input is the movement of the speaker's membrane, which has to be determined from measurements on a laser Doppler vibrometer. The model's output is the sound pressure level at the microphone inside the ear simulator. The calculated results have to be validated with measurements inside the ear simulator. Prototypes of the modelled headphone geometry have to be built for this.

The finite element model is the basis for a headphone development application. The main requirement for this application is, that it can be used easily by non simulation experts to evaluate and optimize the performance of different headphones. This creates several challenges, that have to be considered in the modelling process:

- suitable simplifications have to be found, so that the headphone geometry can be exchanged easily with a minimum of modelling steps required
- pre-defined submodels for a venting hole and an acoustic fleece have to be included, that can be adjusted with simple input parameters
- calculation time has to be kept short, so that different variations of the model can be compared easily

1.3 Approach

The model is created with the simulation software Comsol Multiphysics 5.6. It is divided into three parts: the headphone, the ear simulator and the adapter connecting the headphone with the ear simulator. One specific headphone geometry is used to create and validate the model, always keeping in mind that the geometry must be interchangeable in the final headphone application. Therefore, the submodels for the venting hole and the acoustic fleece are not connected to the headphone part, but to the adapter part. This allows easy use of the predefined submodels for any imported headphone geometry. The ear simulator is replaced by a simplified impedance model. Therefore, the input impedance and the transfer function of the ear simulator are computed. The resulting impedance model is compared to a version with a full model of the ear simulator. The different parts of the model are described in detail in chapter 2.

In order to obtain a valid input signal for the model, the membrane velocity of the loudspeaker is measured with a laser Doppler vibrometer. Another series of measurements is conducted to validate the model's output. For this purpose, the sound pressure level of headphone prototypes is measured in a standardized ear simulator. The measurements are repeated with different insertion depths of the headphone, different venting holes and different acoustic fleeces. The results are used to validate and optimize the Comsol model. All measurements conducted for this work and the comparisons with the simulated results are described in chapter 3.

2

Cmsol Simulation

This chapter describes the finite element model of an in-ear headphone inside a standardized ear simulator. It is the basis for a headphone development application, that is created outside the scope of this work. The application should allow the user to easily import an arbitrary headphone geometry and calculate the SPL inside the ear simulator (see section 1.1). This requirement had to be considered when setting up the model. The validation of the model is carried out in chapter 3.

The model has been built with the software Cmsol Multiphysics 5.6. Section 2.1 will give a short introduction to the software and explain the main features that have been used in the model. Section 2.2 describes the modelled headphone geometry and its resulting Cmsol model. A venting hole and an acoustic fleece are included in the model. As the headphone geometry has to be easily replaceable in the final application, these features are modelled as a part of the adapter without relevant limitations on the validity of the results. Their submodels are therefore discussed together with the model of the adapter for the ear simulator in section 2.3. Different modelling approaches are described and compared to each other.

In section 2.4 the ear simulator and its Cmsol model are presented. As the ear simulator remains unchanged in all simulations in the final application it can be replaced by a boundary condition with its input impedance. The SPL at the microphone inside the ear simulator is then obtained with the help of a transfer function. The calculation of input impedance and transfer function of the ear simulator are explained. A comparison of the simplified impedance model with the full model shows perfect agreement.

2.1 Cmsol Multiphysics

Cmsol Multiphysics is a simulation software based on the finite element method (FEM). It enables the user to model various physical effects and couple different physical domains inside of a model. In this work the *pressure acoustics, frequency domain* interface, which is part of the acoustics module, is used to calculate the acoustic pressure field in the enclosed air volume of a headphone inside of an ear simulator. The model has been built in Cmsol Multiphysics 5.6 running on Windows 10. All the calculations have been done on a computer with 128 GB RAM and an intel xeon E5-1620 v3 processor.

The Cmsol software is well documented. In addition to the general Cmsol introduction manual [2], the *Acoustics Modul User's Guide* [3] is very helpful for understanding the different features that Cmsol offers to model acoustic problems. The explanations are also included in a built-in help system inside the software. Furthermore Cmsol offers a library of example models [4] that guide the user step by step from setting up the model to visualizing the results. Some of these example models will be referred to later on in this chapter when the different parts of the model are explained.

An introduction to the finite element method, different element types and the meshing process in Comsol is given in [5] and will not be repeated in this work. The presented model has been spatially discretised with the automatic meshing feature in Comsol called *physics controlled mesh* in the resolution *finer* (available: extremely coarse, extra coarse, coarser, coarse, normal, fine, finer, extra fine, extremely fine). Very thin parts of the geometry like the venting hole or the acoustic fleece are automatically meshed with smaller elements than larger parts of the model. This feature worked very well for all studied geometries and has therefore been used for all simulations in this work. As an example, the resulting mesh for a model with acoustic fleece and a venting hole ($\varnothing 0.5$ mm, length 3 mm) is shown in figure 2.1. The different parts of the model will be discussed in detail in the following sections.

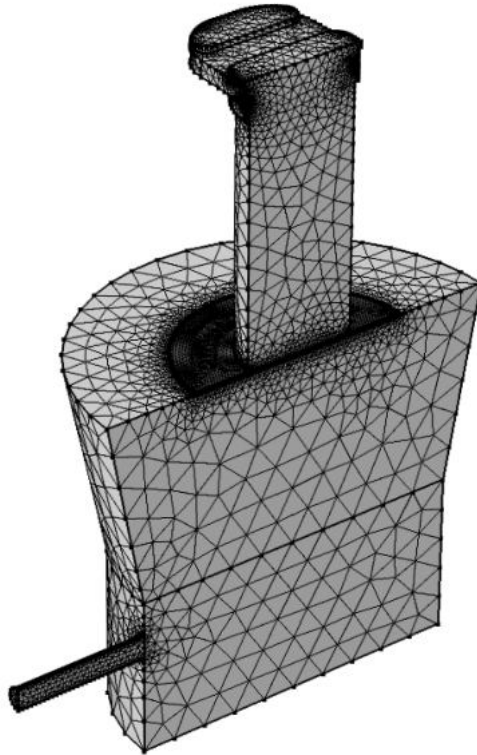


Figure 2.1: Comsol model meshed with automatic meshing feature “*physics controlled mesh*” in the resolution “*finer*”

To calculate the acoustic pressure inside the headphone and the ear simulator, the enclosed air volume has been modelled with the *pressure acoustics, frequency domain* interface. This interface is designed to model the propagation of acoustic waves in the frequency domain. In this case, the air is excited by the oscillating membrane of the loudspeaker. The model is evaluated at a given set of frequencies. For headphone applications the whole human audible frequency range should be covered. Therefore, the model is evaluated at 241 frequency points in the range from 20 Hz to 20 kHz yielding a resolution of $1/24$ octave. For the investigation of the low frequency performance of the venting hole the studied frequency range has been extended downwards to 10 Hz, yielding 265 frequency points.

The *pressure acoustics, frequency domain* interface is based on equation 2.1, an inhomogeneous Helmholtz equation. For the given model it reduces to equation 2.2, because there are no

monopole (Q_m) or dipole (\mathbf{q}_d) sources inside the domain. The acoustic pressure p is assumed to be harmonically oscillating with time according to equation 2.3. As the model is set up in a cartesian coordinate system, the nabla operator ∇ is defined according to equation 2.4. The equations are solved for all discrete points \mathbf{x} of the meshed model. More information about the theoretical background of the pressure acoustics interface in Comsol can be found in [3, p. 224ff.]. For further reading about the Helmholtz equation and its derivation it is referred to [6].

In Comsol, the pressure is denoted as *total acoustic pressure* p_t . It is the sum of the acoustic pressure p and an optional overlaying acoustic background pressure field (see [3, p. 82ff.]). In this work no background pressure field has been applied. The total acoustic pressure p_t therefore equals the acoustic pressure p .

$$\nabla \cdot \left[-\frac{1}{\rho_c} (\nabla p - \mathbf{q}_d) \right] - \frac{\omega^2}{\rho_c c_c^2} p = Q_m \quad (2.1)$$

$$\nabla \cdot \left[-\frac{1}{\rho_c} \nabla p \right] - \frac{\omega^2}{\rho_c c_c^2} p = 0 \quad (2.2)$$

$$p = p(\mathbf{x}, t) = p(\mathbf{x}) e^{i\omega t} \quad (2.3)$$

$$\nabla = \left(\frac{\partial}{\partial x}, \frac{\partial}{\partial y}, \frac{\partial}{\partial z} \right) \quad (2.4)$$

Equation 2.2 requires the density ρ_c and the speed of sound c_c as an input. The subscript c implies, that these quantities can be complex valued. For the lossless case, both ρ_c and c_c are real valued. They become complex, when losses are considered. In this work, losses are considered in the acoustic fleece using the *Poroacoustics* submodel and in the venting hole using the *Narrow Region Acoustics* submodel. These features will be explained in section 2.3.

The material *air* from the Comsol material library is assigned to the whole model. It contains the material data of air depending on the temperature and the absolute pressure. Thus, temperature and absolute pressure have to be defined by the user. For this work the values have always been set to 20 °C and 1 atm. In lossless domains, the values for ρ_c and c_c are directly taken from the *air* material data. In lossy domains, the values are calculated according to the used submodels.

The *linear elastic* fluid model has been selected in the settings of the *pressure acoustics* interface. Thus, the model is lossless except for the areas where special submodels are included, e.g. the venting hole and the acoustic fleece. Table 2.1 summarizes the main settings for the pressure acoustics interface.

Including a model for the thermal and viscous losses inside the acoustic boundary layer for the whole model was not possible here, due to the requirements of the final headphone application. In the following it is explained why the different options, that are available in Comsol to model the losses in acoustic boundary layers, could not be used here.

interface	setting	value
pressure acoustics	material	air
	temperature	20 °C
	absolute pressure	1 atm
	fluid model	linear elastic

Table 2.1: general settings for the modelling interface in Comsol

Thermoviscous acoustics is a separate interface in Comsol. In contrast to the *pressure acoustics* interface, it is based on a more complex set of equations solving not only for the pressure distribution inside the model, but also for the temperature and the three-dimensional velocity field. This approach considers the losses in the acoustic boundary layer without any restrictions on the thickness of the boundary layer or the shape of the model's geometry.

However, this requires a sufficient spatial resolution of the acoustic boundary layer with small mesh elements. Comsol suggests a minimum of ten elements over the thickness of the boundary layer. As the thickness of the acoustic boundary layer is frequency dependent, the mesh of the model should be set up in a frequency dependent way. This results in a quite complex meshing process, that can not be handled by the automatic meshing feature *physics controlled mesh*. The mesh has to be manually adjusted to the modelled geometry.

In the final headphone application the geometry of the headphone has to be easily replaceable by importing an arbitrary geometry. Using the *thermoviscous acoustics* interface therefore would require the end user to set up a complex mesh, taking care of the frequency dependent boundary layer resolution. This is clearly missing the target of a simple user interface, that is designed for non-Comsol users.

The high number of mesh elements required in the boundary layer together with the more complex equations solving for five independent variables instead of one, also yield a much longer calculation time of the model. As calculation time has to be kept short in order to use the final application as a development tool and show it to customers, this is also a big drawback of the *thermoviscous acoustics* approach. Considering these disadvantages the *thermoviscous acoustics* interface is not a feasible option for this task.

Thermoviscous boundary layer impedance is a submodelling feature, that is available in the *pressure acoustics* interface. It is adding an impedance boundary condition at the specified wall, that accounts for the thermal and viscous losses of the acoustic boundary layer. Considering the losses with this boundary condition has two advantages. Firstly, the mesh does not have to be adjusted to resolve the acoustic boundary layer and the automatic meshing feature can still be used. Secondly, this feature is just adding an impedance boundary condition to the Helmholtz equation inside the *pressure acoustics* interface. Therefore, the calculation time does not increase significantly.

The big drawback of this feature is, that it is only valid as long as the acoustic boundary layers of opposite walls are not overlapping. Allowing for an arbitrary, narrow in-ear headphone geometry, this condition can not be fulfilled.

Narrow region acoustics is a submodelling feature, that is available in the *pressure acoustics* interface. Similar to the *thermoviscous boundary layer impedance*, it considers the thermal and viscous losses of the acoustic boundary layer in a compressed way. Adjusting the mesh is not necessary and the calculation time stays almost the same.

The limitation of this feature is the geometry. It is only valid in channels and ducts of constant cross section and can therefore not be used for a general headphone geometry.

The feature is used, however, inside the venting hole and will be discussed in more detail in section 2.3.1.

As non of the available options to model the thermal and viscous losses in the acoustic boundary layer for the whole model are feasible here, the main part of the model has been set up as a lossless model. For the venting hole and the acoustic fleece a suitable submodel to account for the losses is chosen and discussed in section 2.3.

For setting up the model's geometry in Comsol, the *Solidworks Livelink* feature has been used. It couples Comsol with the computer aided design (CAD) software *Solidworks*. Including this feature in the geometry section allows a direct import of the geometry that is currently open in Solidworks into the Comsol model. It is therefore very helpful for the import of different headphone geometries in the final application. The rest of the model's geometry (e.g. the adapter of the ear simulator, the venting hole and the acoustic fleece) is directly defined inside Comsol. The process of setting up geometries in Comsol is well described in [2]. The necessary steps to define the geometry on hand are therefore not described here.

Some of the geometric dimensions have been defined as global parameters (e.g. the radius and the length of the venting hole, the insertion depth of the headphone inside the in-ear adapter) to easily study their influence on the resulting SPL inside the ear simulator. These user-defined parameters will be introduced in the sections about the related parts of the geometry where they are used.

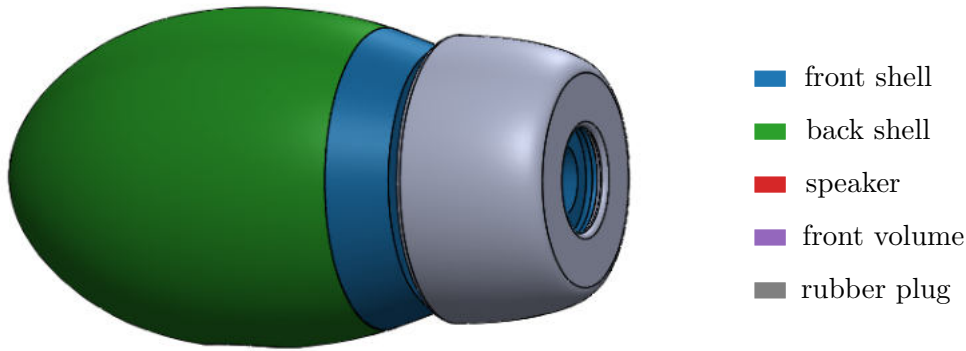
2.2 Headphone Model

This section describes the Comsol model of the in-ear headphone. One specific headphone geometry has been used to set up the model with all necessary boundary conditions. In the final application this headphone geometry is meant to be replaced by an imported geometry using the Comsol *Solidworks Livelink* feature. The simulation settings defined for this prototype however will remain the same, which allows for a very simple user interface. The user just has to select a surface, where the predefined boundary conditions should apply to.

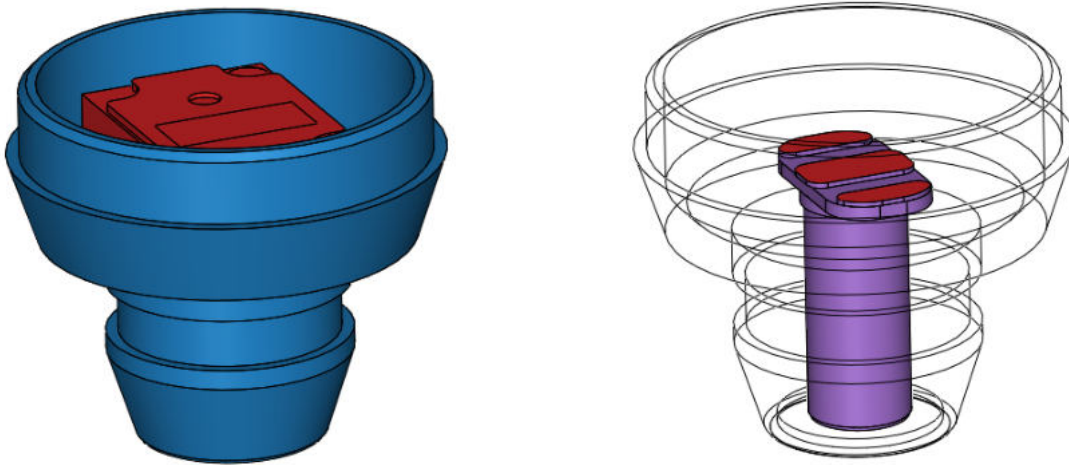
Figure 2.2(a) shows a full CAD model of the used headphone. To avoid modelling the whole loudspeaker, the measured membrane velocity of the speaker is used as an input for the model. Therefore, the model consists only of the part in front of the speaker's membrane. A reduced model, showing only the front shell of the headphone with the loudspeaker, is displayed in figure 2.2(b). The walls of the headphone are assumed to be rigid and sound hard. Therefore only the enclosed air volume is relevant for the simulation. The remaining relevant geometry is the enclosed air volume in front of the loudspeaker's membrane. It is shown in figure 2.2(c).

A prototype of this headphone has been built in order to validate the model by comparing the calculated results with measurements (see section 3.2). The prototype is shown in figure 2.3. The opening areas of the used loudspeaker can be seen in figure 1.1.

Even though this headphone does not include a venting hole, it is a key requirement for the final application to enable the user to analyse the effect of a possible venting hole inside a headphone and to optimize its size. As the headphone geometry will be imported by the user in the final application, modelling the venting hole as a part of the headphone would cause several extra steps for the user to set up the model. Therefore, a parametrized, pre-defined venting model is created inside the adapter part, that is connecting the headphone to the standardized



(a) full CAD model



(b) front shell of the headphone with Achelous speaker (c) air volume in front of the membrane, input surfaces are marked in red

Figure 2.2: in-ear headphone used for the model

ear simulator. By doing this, length and radius of the venting hole can be controlled easily inside the final application, without any extra modelling steps and the headphone's air volume can be imported without a model of the venting hole. The model of the venting hole is discussed in section 2.3.1 .

Shifting the venting hole a few millimetres from the headphone to the adapter part is acoustically negligible, because the venting should only be relevant at very low frequencies. Assuming a cut-off frequency due to the venting hole below the human audible frequency range at approximately 20 Hz, results in a wavelength greater than 17 m. As this wavelength is much greater than the dimensions of the headphone, the location of the venting hole does not have a relevant impact on the results.

Another common feature of in-ear headphones is a thin acoustic fleece on the outlet of the headphone to protect the loudspeaker from dirt. This fleece also has an impact on the acoustic performance of the headphone, which can be used to damp unwanted SPL peaks. Including a

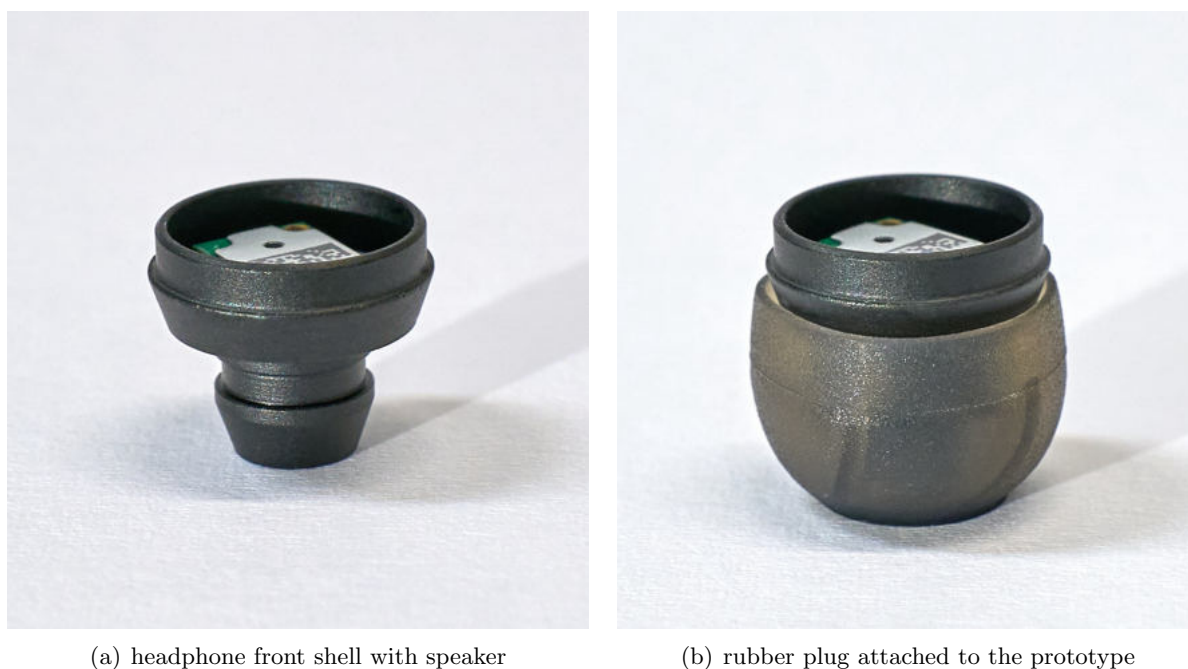


Figure 2.3: headphone prototype

model of such a fleece in the simulation is therefore very important. Following a similar idea as with the venting hole, the submodel for the fleece should not be a part of the changing headphone geometry. As the fleece is usually attached to the outlet of the headphone, its model can also be included on top of the parametrized in-ear adapter instead. This brings the same advantages as previously described for the venting hole: the effect of different fleeces can easily be studied in the final application, no matter which headphone geometry is imported by the user. Furthermore, no additional modelling steps are necessary for the user, as the fleece model is already pre-defined. The submodel of the fleece is discussed in section 2.3.2.

The whole enclosed air volume of the headphone is modelled as a lossless *pressure acoustics* domain (see section 2.1). The boundary condition *normal velocity* is used to model the moving membrane of the loudspeaker as the source of the acoustic waves. The walls of the headphone are modelled with the boundary condition *sound hard wall*. Both of these boundary conditions are described in the following. The settings are summarized in table 2.2.

boundary condition	setting	value
Normal Velocity	amplitude v_n [$\frac{m}{s}$]	$v_in(freq) \cdot \frac{A_{eff}}{A_{in}}$
Sound Hard Wall	-	-

Table 2.2: boundary conditions of the headphone model

normal velocity

The normal velocity boundary condition is used to model the movement of the speaker's membrane, which is the model's input signal. It adds a boundary condition at the selected surface according to equation 2.5, where \mathbf{n} is the normal vector of the selected boundary and v_n is the

user defined velocity amplitude. The surface is assumed to be harmonically oscillating with the studied frequency in the boundary's normal direction.

$$\mathbf{n} \cdot \frac{\nabla p}{\rho_c} = i\omega v_n \quad (2.5)$$

The frequency dependent membrane velocity amplitude has been obtained from measurements of ten speakers on a laser Doppler vibrometer in the range from 20 Hz to 20 kHz with a resolution of $1/12$ octave. The measurements are described in section 3.1. The averaged velocity data is stored in a local table inside the Cmsol model. In order to evaluate the model at any given frequency, an interpolation function `v_in(freq)` is defined for the velocity data. The variable `freq` is a pre-defined Cmsol variable, that stores the frequencies that the model is solved for. The amplitudes at studied frequencies between the measured data points are linearly interpolated. For studying the low frequency behaviour of the venting hole, the velocity data table has been manually extrapolated downwards to 10 Hz, following the decay in amplitude by a factor of two per frequency octave towards low frequencies.

The *normal velocity* boundary condition is applied to the opening surfaces of the loudspeaker (see figure 2.2(c)). The surface area of these boundaries is not equal to the surface area of the speaker's membrane. It is assumed, that the air volume that is moved by the speaker's membrane is the same as the air volume that is moved through the speaker's openings. Therefore, the measured membrane velocity has to be scaled by the ratio of the membrane area and the selected boundary area.

It also has to be considered, that the speaker's membrane is not moving like a planar plate, as it is modelled by the *normal velocity* boundary condition. The edges of the membrane are fixed and therefore the velocity is decreasing towards the edges. The velocity has been measured at the centre point of the membrane. A corresponding effective membrane area is available in the company's database. The effective membrane area is the area of a planar plate moving with the membrane's centre point velocity, that yields the same volume velocity as the real membrane.

In order to implement the described calculation, the variables A_{eff} and A_{in} are defined in the model. A_{eff} holds the fixed value of 11.9 mm^2 for the effective membrane area of the speaker. The area of the modelled input surface A_{in} has to be calculated according to the selected input boundaries in the imported headphone geometry. For this reason the integral function `int_in(x)` has been defined. It returns the integral of its argument over the selected input boundaries. The surface area A_{in} is then obtained by the expression `int_in(1)`. The velocity amplitude v_n in the *normal velocity* settings is defined according to equation 2.6. If only half of the headphone is modelled due to symmetry, the modelled input surface has to be multiplied by two or the effective membrane area has to be divided by two in order to obtain the correct scaling. The defined variables and functions are summarized in table 2.3.

$$v_n = \text{v_in}(freq) \cdot \frac{A_{eff}}{A_{in}} \quad (2.6)$$

In the final application, the input surface of the imported headphone geometry has to be selected by the user. The pre-defined *normal velocity* boundary condition, as it is described here, is then automatically applied to the selected boundary. The surface integral `int_in(1)` is evaluated on the selected boundary and the scaling factor A_{eff}/A_{in} is calculated accordingly.

variable/function	value	description
$freq$	10 Hz...20 kHz	array of studied frequencies (1/24 oct)
A_{eff}	11.9 mm ²	effective membrane area of the speaker
A_{in}	int_in(1)	modelled input surface in m ²
int_in(\mathbf{x})	$\int_{A_{in}} x dA$	integral of function's argument over the selected input surface
v_in($freq$)	m/s	measured membrane velocity (1/12 oct) interpolated at the studied frequencies (1/24 oct)

Table 2.3: variables and functions used in the headphone model

sound hard wall

This boundary condition is used on all boundaries of the headphone geometry except of the input surface. It assumes rigid walls, that do not vibrate. For the case at hand without a dipole domain source ($\mathbf{q}_d = 0$) and for constant density of air ρ_c inside the headphone, this boundary condition results in equation 2.7. It means, that the derivative of the acoustic pressure in the boundary's normal direction \mathbf{n} is zero at the wall.

$$\frac{\partial p}{\partial \mathbf{n}} = 0 \quad (2.7)$$

Mathematically this expression is identical to the symmetry condition inside the pressure acoustics interface. Thus, for symmetric models this boundary condition can also be used on the symmetry plane.

2.3 Adapter Model

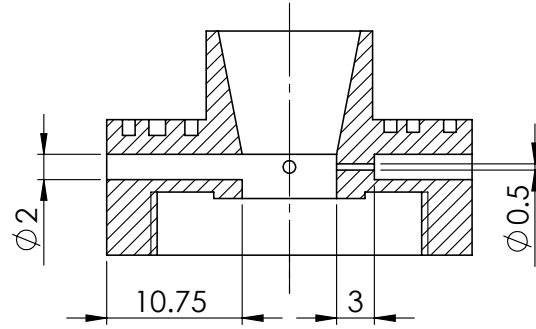
To connect the in-ear headphone with the ear simulator, a cone-shaped adapter has to be used. The adapter is screwed on top of the ear simulator. The headphone is then plugged into the adapter as it would be plugged into the opening of a human ear canal. In this work, two different adapters are used: the GRAS RA0088 in-ear adapter and a special made leakage adapter. The main air volume of the leakage adapter is identical to the air volume of the GRAS in-ear adapter, but it contains four thin holes with different diameters. It has been created to study the influence of different venting holes on a given headphone. The two adapters are shown in figure 2.4(a).

Figure 2.4(b) shows a vertical section of the leakage adapter. The four different venting holes are distributed over the adapter's rim in 90° angles. All four holes are 10.75 mm long, but only the widest hole with a diameter of 2 mm has constant cross-section over the full length. The other holes, with diameters of 0.2 mm, 0.5 mm and 1 mm, include a jump in cross-section after a length of 3 mm to the diameter of 2 mm. This was necessary due to production restrictions.

When measuring with the leakage adapter, three of the holes are alternately closed so that only one hole is open at a time. As the main air volumes of the adapters are identical, the two adapters can be summarized in one model with an optional parametrized venting hole. This section describes the resulting model of the adapter. The submodel for the venting holes is discussed in subsection 2.3.1.



(a) GRAS RA0088 in-ear adapter (left) and special made leakage adapter (right)



(b) drawing of leakage adapter, dimensions in *mm*

Figure 2.4: in-ear headphone adapters for the ear simulator

The model also includes a submodel for an acoustic fleece, that is usually added at the outlet of an in-ear headphone. In the final application it has to be easy to study the effect of different acoustic fleeces for any imported headphone geometry. Therefore, the submodel of the fleece is decoupled from the imported headphone geometry and included on top of the adapter. This does not change the location of the fleece, being at the outlet of the headphone. But it allows to define a parametrized model of the fleece, that can be used without any extra modelling steps on the imported headphone geometry. In order to cover also headphones with a larger outlet diameter than the presented headphone model, the diameter of the fleece model is chosen to be larger than the headphone used in this work. The submodel for the acoustic fleece is discussed in subsection 2.3.2.

In contrast to the headphone's geometry, which is imported from Solidworks, the adapter's geometry is built directly in Cansol. The metal walls of the adapter are assumed to be rigid and sound hard. Therefore, only the enclosed air volume inside the adapter is modelled. The diameter jump between the headphone outlet and the adapter inlet is modelled as a plane surface terminating the adapter's air volume on top. This corresponds to the assumption of a perfectly plane sealing by the rubber plug. Instructions on how to set up a geometry in Cansol are given in [2]. The resulting model is shown in figure 2.5.

The air volume of the adapter is modelled as a pressure acoustics domain, resulting in a lossless propagation of sound. Inside of the venting hole a model for the losses in the acoustic boundary layer is included with the *Narrow Region Acoustics* feature. The venting hole is terminated with an impedance boundary condition for unflanged circular pipes. The acoustic fleece is modelled as a separate domain with the *Poroacoustics* feature using the Delany-Bazley model. The walls of the adapter are modelled with the *Sound Hard Wall* boundary condition according to equation 2.7, yielding a vanishing derivative of the acoustic pressure in the boundary's normal direction at the wall. For the calculations in this work, the model's symmetry has been exploited. The resulting symmetry plane is also modelled with the *Sound Hard Wall* boundary condition.

The ear simulator is connected at the bottom surface of the adapter. To reduce the model's complexity an impedance boundary condition with the ear simulator's input impedance is defined here. The definition and calculation of this impedance is explained in section 2.4.

Some geometric dimensions have to be adjustable by the user in the final application in order

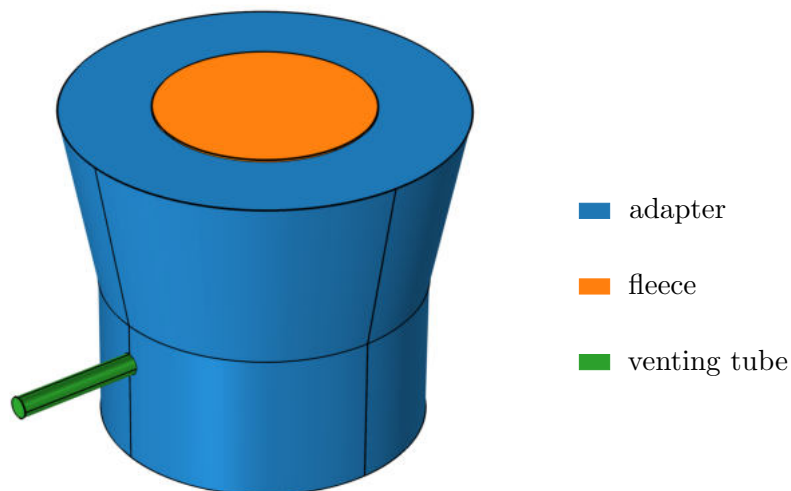


Figure 2.5: Comsol model of the in-ear adapter for the ear simulator with venting hole and acoustic fleece

to study variations of the venting hole and the insertion depth of the headphone. Therefore, these parameters are defined as global variables in the model, that can later be accessed and used in the Comsol application builder. Furthermore the variables are used to validate the model for different venting sizes and insertion depths. The validation of the model is described in section 3.2.

The variable h_{insert} controls the insertion depth of the headphone by decreasing the height of the remaining air volume in the adapter accordingly. As the cone-shaped part is 9.3 mm high, valid values have to be in the range: $0\text{ mm} < h_{insert} < 9.3\text{ mm}$. The model is studied and validated for four different values of the insertion depth, as shown in table 2.4. The defined variables for the acoustic fleece and the venting hole are introduced in the following subsections together with the corresponding submodels.

variable	value	description
h_{insert}	4/5/6/7 mm	insertion depth of the headphone

Table 2.4: user defined variable with its studied values to control the geometry of the adapter

2.3.1 venting hole

The venting hole is modelled inside of the adapter for the ear simulator, at the same location where it is in the leakage adapter (see figure 2.4). Therefore, the model can be validated with the four available venting sizes in the leakage adapter ($\varnothing 0.2\text{ mm}$, $\varnothing 0.5\text{ mm}$, $\varnothing 1\text{ mm}$, $\varnothing 2\text{ mm}$). For the validation three holes of the leakage adapter are alternately closed, while length and radius of the venting model are adjusted to the size of the open hole. As the venting is especially important at low frequencies, the frequency range has been extended downwards to 10 Hz for the study of the venting behaviour. The model's validation is described in section 3.2.3.

As described in section 2.2, the venting hole is actually a part of the headphone. Modelling

it in the adapter is necessary in order to meet the requirements of the final headphone application. Different venting holes have to be studied for an arbitrary user-imported headphone geometry with a minimum of modelling steps. This is possible with the pre-defined venting model, that is presented in this section. It allows the user to easily change the venting hole or disable it completely without any modelling experience required. The cut-off frequency of the headphone's SPL due to the venting is typically designed to be at the lower end of the human audible frequency range. The wavelength at the cut-off frequency is then much larger than the distance between the headphone and the adapter. Therefore, modelling the exact location of the venting hole is acoustically not very important.

As the venting hole is a very thin tube, the influence of the acoustic boundary layer has to be considered. Inside of this area relevant losses appear due to high gradients of temperature and velocity close to the wall (see [7]). The thickness of the boundary layer is frequency dependent. It also depends on the material parameters of the fluid. The thickness of the acoustic boundary layer caused by viscous and thermal effects can be approximated separately according to [8, p. 19f.] by the equations 2.8. In [7] the acoustic boundary layer is defined as half of the viscous wavelength, resulting in a thickness $\delta = \pi \cdot \delta_{visc}$. As Cmsol also refers to the equations 2.8 (see [9]), this definition is used in this work.

$$\delta_{visc} = \sqrt{\frac{\mu}{\pi f \rho_0}} \quad \delta_{therm} = \sqrt{\frac{k}{\pi f \rho_0 C_p}} \quad (2.8)$$

The equations are evaluated for air at 20 °C and 1 atm using the following material parameters. The results are visualized in figure 2.6.

material parameter	value
density ρ_0	1.2 kg/m ³
dynamic viscosity μ	1.83 · 10 ⁻⁵ kg/m·s
thermal conductivity k	0.025 W/m·K
specific heat capacity C_p	1007 J/kg·K

Table 2.5: material parameters for air at 20 °C

It can be seen in figure 2.6 that the thermal and the viscous boundary layer thicknesses are comparable in air. For other fluids this might not be the case. It can also be observed, that especially for very thin venting holes, e.g. \varnothing 0.2 mm, the boundary layer takes already at high frequencies an important fraction of the hole's diameter. At low frequencies the opposite boundary layers are even overlapping. For the \varnothing 0.2 mm hole the overlapping starts already at 500 Hz.

The *Narrow Region Acoustics* feature inside the pressure acoustics domain is designed to model the losses in the acoustic boundary layer. It makes use of analytical solutions for the losses in simple geometries with constant cross-section. Therefore, the model is still solving the Helmholtz equation (see equation 2.2), while the speed of sound and the density are calculated according to the analytical loss model and become complex valued inside the *Narrow Region*. This feature is computationally very efficient and is therefore well suited for the final application, where calculation time is an important parameter. It neither requires a fine spacial resolution of the acoustic boundary layer nor a calculation of the temperature distribution and the three dimensional velocity field inside the venting hole.

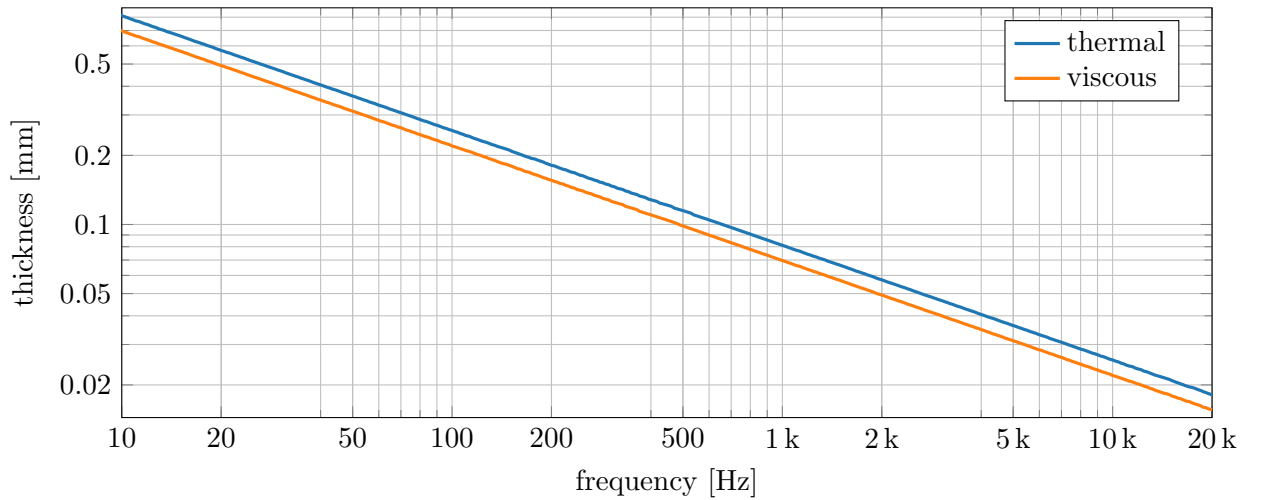


Figure 2.6: viscous and thermal boundary layer thickness according to equations 2.8 using the material parameters of air given in tabel 2.5.

In the settings of the *Narrow Region Acoustics* feature, the *duct type* can be selected. As the venting hole has a circular cross-section, the *circular duct* model is chosen. With this choice, the analytical loss model is defined according to equations 2.9 - 2.11. The model is valid if the acoustic wavelength is much larger than both the cross-section of the hole and the boundary layer thickness (see [3, p. 280ff.]). The highest studied frequency is 20 kHz yielding a minimum wavelength of approximately 1.7 cm. Compared to the widest studied venting hole (\varnothing 2 mm) and the acoustic boundary layer thickness (see figure 2.6), this condition is clearly fulfilled. According to the Comsol manual, the *Narrow Region Acoustics* feature is therefore valid for the venting hole over the full studied frequency range, covering overlapping as well as non-overlapping acoustic boundary layers.

$$c_c = c \cdot \sqrt{\frac{Y_v}{\gamma - (\gamma - 1)Y_{th}}} \quad , \quad \rho_c = \frac{\rho}{Y_v} \quad (2.9)$$

$$Y_v = -\frac{J_2(ak_v)}{J_0(ak_v)} \quad , \quad Y_{th} = -\frac{J_2(ak_{th})}{J_0(ak_{th})} \quad (2.10)$$

$$k_v^2 = -i\omega \frac{\rho}{\mu} \quad , \quad k_{th}^2 = -i\omega \frac{\rho C_p}{k} \quad (2.11)$$

The equations require knowledge of the following material data of the fluid inside the duct: speed of sound c , density ρ , ratio of specific heats γ , dynamic viscosity μ , specific heat capacity C_p and thermal conductivity k . The values are taken from the material *air* in the Comsol material library for the modelled temperature of 20 °C and an absolute pressure of 1 atm. The variable a in the argument of the Bessel functions J_0 and J_2 is the only input parameter of the *Narrow Region* feature. It is the radius of the modelled circular duct. In this work, the defined global variable for the radius of the venting hole can be used to set $a = r_{venting}$.

The venting hole opens into free space. Therefore, a finite model of the infinite space around the headphone is necessary. A simple and computationally efficient way to do this is to define

a suitable impedance boundary condition to terminate the hole. For the case at hand without dipole domain sources ($\mathbf{q}_d = 0$), an impedance boundary condition is defined in Comsol according to equation 2.12. \mathbf{n} is boundary's normal vector and Z_i is the acoustic input impedance of the external domain in $Pa \cdot s/m$, that has to be defined by the user.

$$\mathbf{n} \cdot \frac{\nabla p}{\rho_c} = -\frac{i\omega p}{Z_i} \quad (2.12)$$

Comsol offers a selection of pre-defined impedance models to consider the frequency dependent radiation of an opening into free space. The so-called *waveguide end impedance* models are available for flanged and unflanged openings (see [3, p. 252f.]). A flanged opening radiates into a semi-infinite space, while the radiation of an unflanged opening is omni-directional. The difference of the flanged and the unflanged impedance condition is illustrated in the Comsol tutorial model *Open Pipe* [10].

For the case of a vented headphone, an unflanged model for the opening should be chosen. When the headphone is plugged into the ear, the opening of the venting is “flanged” only to the human head. As the venting is usually designed for frequencies at the lower end of the human audible frequency range, the relevant wavelength for radiation is several meters long. Compared to this wavelength, the human head is very small and the waves are bent around it. The radiation is therefore better approximated with an unflanged opening.

Another important parameter for determining the best fitting impedance model is the product ka of wave number and opening radius. The studied frequency range (10 Hz - 20 kHz) and the analysed venting sizes ($\varnothing 0.2 \text{ mm}$ - $\varnothing 2 \text{ mm}$) yield values for ka in the range from $1.8 \cdot 10^{-5}$ to 0.37. As $ka \ll 1$ is fulfilled over the whole range of studied frequencies and geometries, the *unflanged pipe, circular (low ka limit)* impedance model can be applied to the circular opening of the venting hole. The impedance is defined according to equation 2.13 (see [3, p. 253]) and visualized in figure 2.7.

$$Z_{end} = \rho c \left[\frac{(ka)^2}{4} + i \cdot 0.6133 \cdot ka \right] \quad (2.13)$$

As the venting hole is modelled with the *Narrow Region Acoustics* feature, the pre-defined *unflanged pipe, circular (low ka limit)* impedance model Z_{end} can not be used directly for the definition of the boundary impedance Z_i in equation 2.12 at the outlet of the venting hole. Inside the *Narrow Region*, the values of ρ and c are changed to ρ_c and c_c according to equation 2.9 in order to model the losses in the hole. Comsol is using these values to calculate the end impedance at the boundary. This is an unexpected behaviour, as the end impedance for radiation into free space should only depend on the opening surface and the properties of the outer domain. By using the adjusted quantities from the *Narrow Region*, the impedance depends on the properties of the inner domain. Thus, the calculated end impedance changes when the *Narrow Region* feature inside the venting hole is disabled.

To avoid this unwanted behaviour, the end impedance for unflanged circular pipes at low ka is implemented as a user defined impedance Z_i as shown in equation 2.14. The equation is identical to equation 2.13, but the values for the density ρ and the speed of sound c are fixed to $\rho = 1.2 \text{ kg/m}^3$ and $c = 343 \text{ m/s}$. The wave number k therefore is replaced by the expression ω/c , while the currently studied angular frequency ω is referred to by the Comsol internal variable *acpr.omega*. For the opening radius a the user defined variable *r_venting* is inserted. With this implementation the desired end impedance is calculated correctly and can be used in the model,

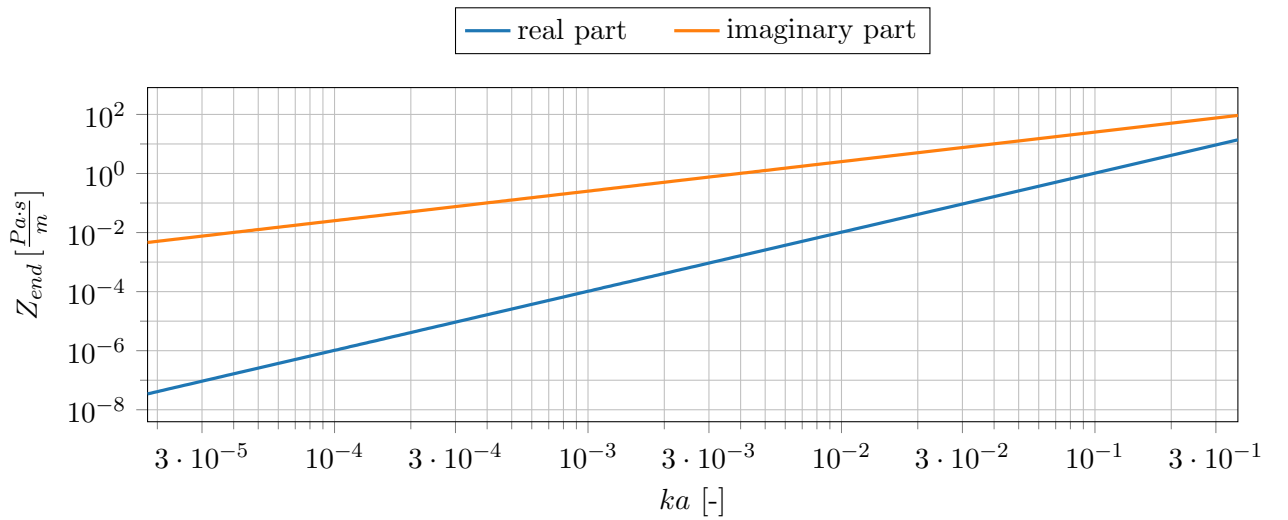


Figure 2.7: end impedance of the venting hole for an unflanged circular pipe at $ka \ll 1$

even though it is terminating a *Narrow Region*. Equation 2.14 is applied for all venting studies in this work.

$$Z_i = 1.2 \left[\frac{kg}{m^3} \right] \cdot 343 \left[\frac{m}{s} \right] \cdot \left[\frac{1}{4} \left(\frac{acpr.omega}{343 \left[\frac{m}{s} \right]} \cdot r_{venting} \right)^2 + i \cdot 0.6133 \cdot \frac{acpr.omega}{343 \left[\frac{m}{s} \right]} \cdot r_{venting} \right] \quad (2.14)$$

Out of the four studied holes of the leakage adapter only the $\varnothing 2$ mm hole has constant cross-section over the full length of 10.75 mm (see figure 2.4(b)). The three smaller holes include a jump in cross-section after a length of 3 mm. As the *Narrow Region* feature only applies to areas of constant cross-section, two modelling approaches for these holes are presented here:

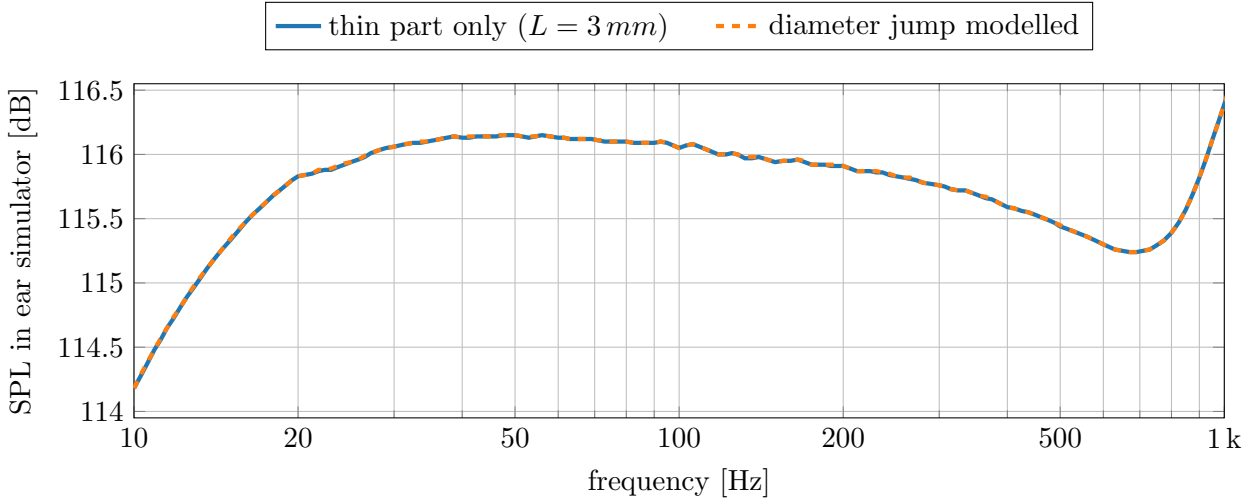
- The thin and the wide part of the venting hole are modelled with two different *Narrow Region* domains. The *circular duct* model according to equations 2.9 - 2.11 is applied to both parts with the corresponding radius. The open end of the wide part of the hole is terminated with the presented impedance boundary condition according to equation 2.14.
- Only the thin part of the venting hole previous to the diameter jump is considered and modelled with the presented *Narrow Region* model. At the position of the jump, the impedance boundary condition according to equation 2.14 is applied. This simplification assumes the jump from the thin part to the wide part of the hole to be so large that it behaves like an open end into free space.

The SPL inside the ear-simulator is compared for the two models in figure 2.8(a) for the $\varnothing 0.2$ mm hole. The results are computed with the headphone model described in section 2.2 ($h_{insert} = 5$ mm), the ear simulator's input impedance boundary condition as described in section 2.4 and without acoustic fleece. It can be seen that the two models match perfectly. Neglecting the wide part behind the diameter jump and modelling the thin part only is therefore a reasonable simplification. The following results in this work are computed with this simplification, applying the end impedance directly at the location of the diameter jump ($L = 3$ mm) for the three thin holes. The $\varnothing 2$ mm hole with constant cross-section is modelled with the full length of 10.75 mm.

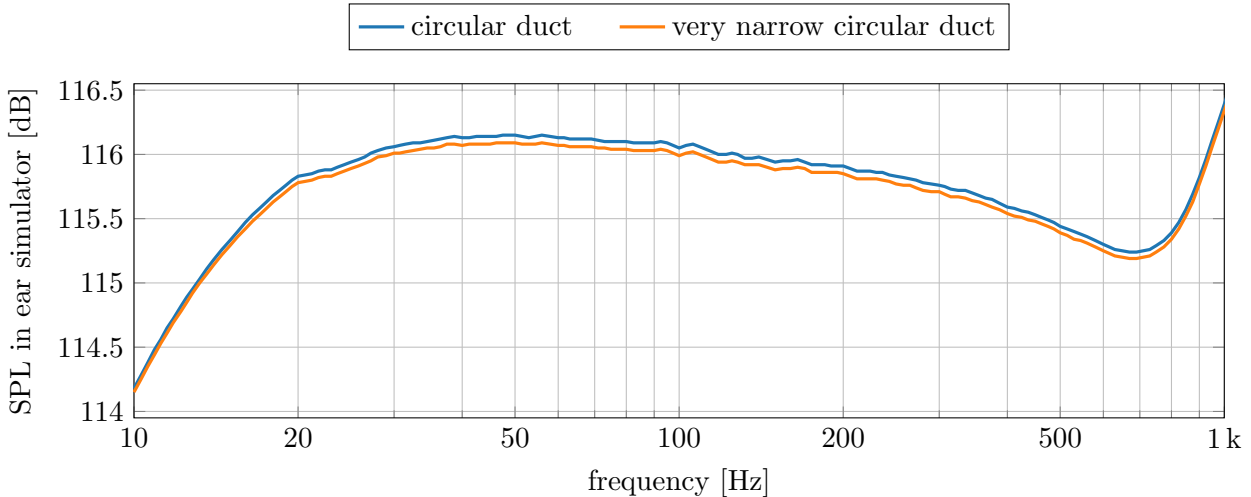
Table 2.6 lists the user defined and Comsol internal variables, that are used in the venting model together with their studied values:

variable	value	description
$r_{venting}$	0.1/0.25/0.5/1 mm	radius of the venting hole
$L_{venting}$	3/10.75 mm	length of the venting hole
$acpr.omega$	$2\pi \cdot freq$	currently studied angular frequency

Table 2.6: user defined variables for the geometry of the venting hole and their tested values



(a) influence of modelling the diameter jump inside the venting hole after $L = 3\text{ mm}$ for the $\varnothing 0.2\text{ mm}$ hole



(b) comparison of different *Narrow Region* loss models for the smallest venting hole ($\varnothing 0.2\text{ mm}$, $L = 3\text{ mm}$)

Figure 2.8: comparison of different modelling approaches for the venting hole in Comsol

For the thinnest hole ($\varnothing 0.2\text{ mm}$) another comparison is conducted in order to see the performance of the *Narrow Region* loss model for overlapping acoustic boundary layers. The presented *circular duct* loss model is replaced by the *very narrow circular duct (isothermal)* model in the *Narrow Region* settings. While the *circular duct* model is valid for overlapping as well as non-overlapping acoustic boundary layers, the isothermal model is only valid if the acoustic boundary layer thickness is much larger than the hole's diameter [3, p. 281]. For the $\varnothing 0.2\text{ mm}$ the acous-

tic boundary layer is larger than the hole's diameter for frequencies below 100 Hz (see figure 2.6).

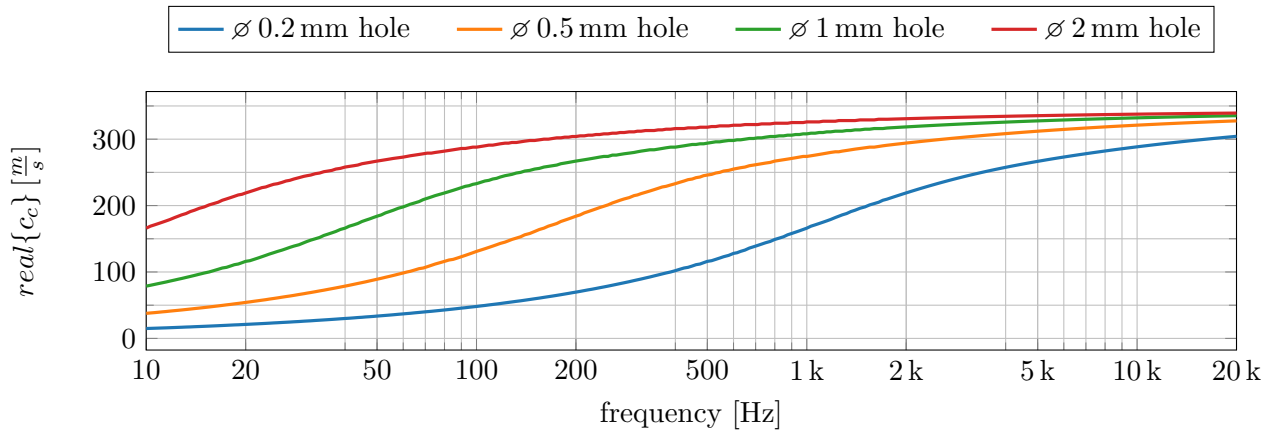
The SPL inside the ear-simulator is calculated for both models and visualized in figure 2.8(b). The previously discussed simplification is used, so only the thin part of the venting hole with a length of 3 mm is modelled. The difference of the two models is less than 0.1 dB over the whole range from 10 Hz - 1 kHz. This means that there is no need to switch to the *very narrow circular duct (isothermal)* model for the thinnest hole. The *circular duct* loss model is therefore used for all following venting studies.

The relevant settings in Comsol for the venting model are summarized in table 2.7. The resulting speed of sound and density inside the venting hole are calculated with these settings and visualized in figure 2.9. As discussed earlier, these quantities become complex valued inside the *Narrow Region* domain to account for the losses. According to equation 2.9 the speed of sound and the density inside the venting hole are independent of the position inside the hole and assumed to be constant over the full length.

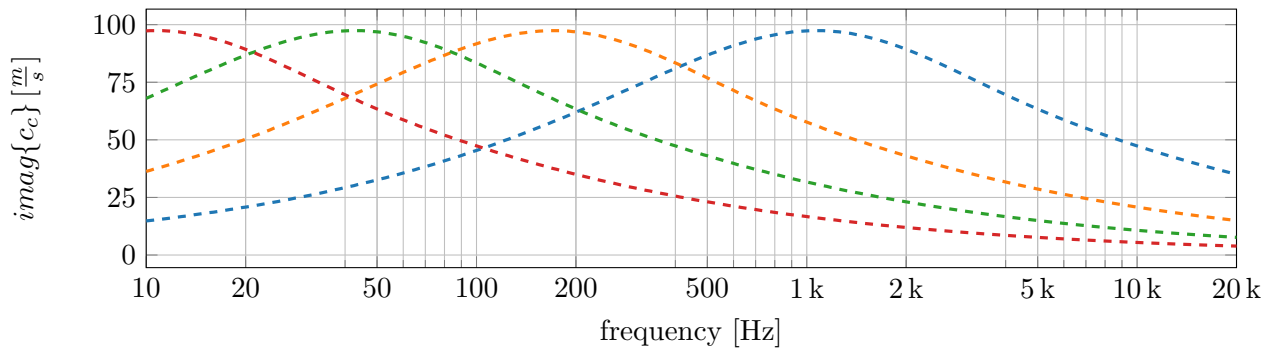
For wider holes and higher frequencies the fraction of the acoustic boundary layer in the hole becomes smaller and therefore the acoustic behaviour becomes more similar to a lossless wave propagation. This effect can be observed in the plots of c_c and ρ_c : At high frequencies the imaginary parts are diminishing and the real parts are approaching the standard values of $c = 343 \text{ m/s}$ and $\rho = 1.2 \text{ kg/m}^3$. A wider hole shifts this process towards lower frequencies.

used feature	setting	value
Narrow Region Acoustics	duct type	circular duct
	radius	$r_{venting}$
Impedance Boundary Condition	user defined impedance $Z_i \left[\frac{\text{Pa}\cdot\text{s}}{\text{m}} \right]$	$\rho c \left[\frac{(ka)^2}{4} + i \cdot 0.6133 \cdot ka \right]$

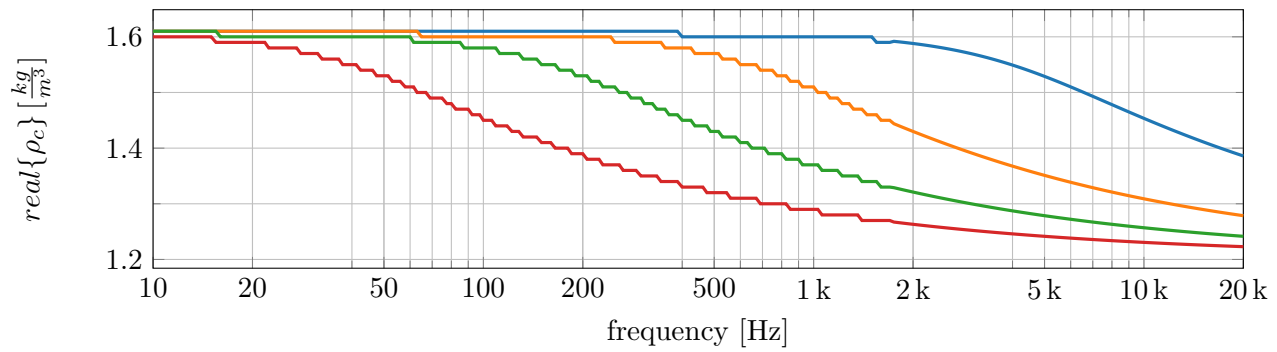
Table 2.7: relevant settings in Comsol for the venting model



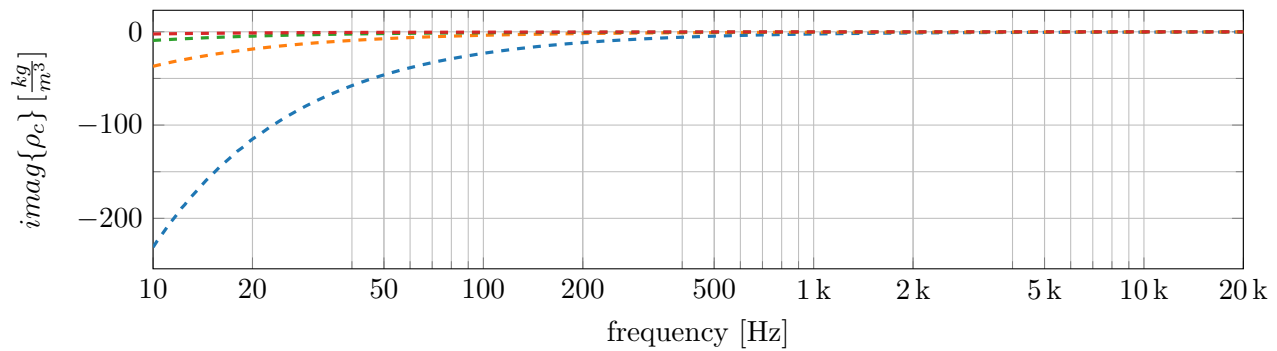
(a) real part of speed of sound



(b) imaginary part of speed of sound



(c) real part of density



(d) imaginary part of density

Figure 2.9: complex valued speed of sound c_c and density ρ_c inside the narrow region domain of the different venting holes

2.3.2 acoustic fleece

This section describes the submodel of an acoustic fleece, that is added at the outlet of the in-ear headphone. A fleece is used to protect the speaker from mechanical damage and dirt. At the same time it is acoustically relevant to optimize the SPL response of the headphone inside the ear simulator. The fleece is modelled as a separate domain on top of the adapter in order to use the defined fleece model for any imported headphone geometry.

The *Poroacoustics* feature is used in Comsol to calculate the wave propagation inside the acoustic fleece. It provides several models for porous materials that need different input parameters. Many of these input parameters require a deep knowledge about the porous material and are hard to determine. For this work, the acoustic fleeces from the Saati Acoustex collection should be used, as they are typically used on the headphones in the company. With the available material data about these fleeces [11] only the Delany-Bazley model can be chosen.

The Delany-Bazley model is an empirical one-parameter model that only needs the material's airflow resistivity R_f [$\text{Pa}\cdot\text{s}/\text{m}^2$] as an input. It is based on the equations 2.15 and 2.16 for the complex valued wave number k_c and impedance Z_c inside the porous material. These polynomials make use of the dimensionless normalized frequency X according to equation 2.17. They are fitted to measured data with a set of eight coefficients $C_1 \dots C_8$. Different fittings can be found in the literature yielding different coefficients. In Comsol, nine different fittings are available. The corresponding coefficient sets are listed in table 2.8.

$$k_c = \frac{\omega}{c} \cdot [1 + C_1 X^{-C_2} - i C_3 X^{-C_4}] \quad (2.15)$$

$$Z_c = \rho c \cdot [1 + C_5 X^{-C_6} - i C_7 X^{-C_8}] \quad (2.16)$$

$$X = \frac{f \cdot \rho}{R_f} \quad (2.17)$$

fitting	C_1	C_2	C_3	C_4	C_5	C_6	C_7	C_8
Delany-Bazley	0.0978	0.7	0.189	0.595	0.0571	0.754	0.087	0.732
Miki	0.122	0.618	0.18	0.618	0.079	0.632	0.12	0.632
Qunli	0.188	0.544	0.163	0.592	0.209	0.548	0.105	0.607
glass fiber, low X	0.135	0.646	0.396	0.458	0.0688	0.707	0.196	0.549
glass fiber, high X	0.102	0.705	0.179	0.674	0.0235	0.887	0.0875	0.77
rock fiber, low X	0.136	0.641	0.322	0.502	0.081	0.699	0.191	0.556
rock fiber, high X	0.103	0.716	0.179	0.663	0.0563	0.725	0.127	0.655
Komatsu	0.0004	-6.2	0.0069	-4.1	0.00027	-6.2	0.0047	-4.1
Champoux/Allard	0.0982	0.685	0.288	0.526	0.0729	0.66228	0.187	0.5379

Table 2.8: available coefficient sets for the Delany-Bazley model in Comsol

Four different fleeces from the Saati Acoustex collection are chosen for the investigations in this work. The fleeces are spanning the range from $42 \text{ Pa}\cdot\text{s}/\text{m}$ to $260 \text{ Pa}\cdot\text{s}/\text{m}$, which is the relevant airflow resistance range for the company's headphone applications. An extract from the data

sheet of the used acoustic fleeces is shown in table 2.9. It has to be noted that the values given in the data sheet are not material parameters, but refer to the fleece as a finished product. The quantity is called airflow resistance and it is given in the unit $Pa \cdot s/m$. In contrast, the input parameter of the Delany-Bazley model is a material dependent quantity of the unit “airflow resistance per length”. It is called airflow resistivity.

fleece	airflow resistance [$Pa \cdot s/m$]	open area [%]	thickness [μm]
Acoustex 042	42	29	46
Acoustex 080	80	27	44
Acoustex 160	160	15	58
Acoustex 260	260	13	60

Table 2.9: extract from data sheet of the used acoustic fleeces from Saati [11]

In order to implement the Delany-Bazley model in a user friendly way, three additional variables are defined. The value of the variable $R_{f,tot}$ is entered directly by the user. It contains the airflow resistance of the studied fleece as it is given in the data sheet. The variable d_{fleece} defines the thickness of the acoustic fleece. It is used to calculate the airflow resistivity R_f and also to specify the thickness of the poroacoustic domain in the model. This variable could be adjusted with another user input to the thickness of the different fleeces. It has been decided, however, to model all of the fleeces with a thickness of $d_{fleece} = 50 \mu m$ in order to keep the user interface of the final headphone development application as simple as possible. For the used fleeces this is a good approximation (see table 2.9). The defined variables are summarized in table 2.10.

variable	value	description
d_{fleece}	$50 \mu m$	thickness of acoustic fleece
$R_{f,tot}$	$42/80/160/260 Pa \cdot s/m$	total airflow resistance of acoustic fleece
R_f	$R_{f,tot}/d_{fleece}$	airflow resistivity of fleece material in $Pa \cdot s/m^2$

Table 2.10: internal and user-generated variables used in the model

The variable R_f is used to set up a new user defined material for the acoustic fleece. As the airflow resistivity is the only parameter of the porous material that is needed by the Delany-Bazley model, the material definition contains only this value. The new material is called “acoustic fleece” and it is assigned to the poroacoustic domain. The material of the fluid inside the pores of the fleece also has to be specified in the settings of the *Poroacoustics* feature. The material *air* from the Cmsol library is selected here. The settings for the poroacoustic model of the fleece are summarized in table 2.11.

used feature	setting	value
	poroacoustic model	Delany-Bazley
Poroacoustics	fluid material	air (Cmsol library)
	porous elastic material	acoustic fleece (user defined)

Table 2.11: relevant settings in Cmsol for the fleece model

The validity of the Delany-Bazley model is restricted to highly porous materials with a porosity close to one. As it can be seen in table 2.9, the open area and thus the porosity of the used fleeces is much smaller than one. As there is not enough material data to use any other porous model for the fleece, this drawback has to be accepted here. The different coefficient sets add further limitations regarding the valid frequency and airflow resistivity range. In the following the applicability of the different coefficient sets is discussed.

The applicability of the different fittings in Comsol is given in [3, p. 271ff.] and summarized in table 2.12. To evaluate these criteria, it is necessary to compute the minimum and the maximum airflow resistivity that is used as an input for the Delany-Bazley model. For the selected fleeces listed in table 2.9 and the defined thickness $d_{fleece} = 50 \mu m$ of the porous domain the values are calculated as:

$$R_{f,min} = \frac{42 \frac{Pa \cdot s}{m}}{50 \mu m} = 8.4 \cdot 10^5 \frac{Pa \cdot s}{m^2}$$

$$R_{f,max} = \frac{260 \frac{Pa \cdot s}{m}}{50 \mu m} = 5.2 \cdot 10^6 \frac{Pa \cdot s}{m^2}$$

With these results, the given limitations on the normalized frequency X can be transformed into a valid frequency range according to equation 2.18. The results are included in table 2.12.

$$f_{min/max} = \frac{X_{min/max} \cdot R_{f,max/min}}{\rho} \quad (2.18)$$

The fittings from Delany-Bazley, Miki, Qunli and Komatsu can not be used in any frequency range because the airflow resistivity of the selected fleeces exceeds the specified validity range. The Mechel high X fittings apply only to frequencies far beyond the audible frequency range and are therefore not suitable for headphone applications. The Mechel low X fittings and the Modified Champoux and Allard coefficients cover the audible frequency range quite well. These fittings are therefore considered as possible modelling options for the acoustic fleece. It has to be noted, however, that the Mechel coefficients are designed for glass and rock fiber while the Saati Acoustex fleeces are made from polyester monofilament fiber. In section 3.2.4 the simulated results with the three selected coefficient sets are compared to measurements.

In order to see the effect of valid and invalid coefficient sets on the model's output, the SPL at the microphone membrane inside the ear simulator is calculated for all nine fittings of the fleece model. For the calculation, the headphone model as described in section 2.2 and the ear simulator impedance boundary condition as described in section 2.4 are used. The insertion depth of the headphone is set to $h_{insert} = 5 mm$ and no venting is applied.

The results are shown in figure 2.10. As the fleece does not have a relevant impact on the frequencies below 5 kHz, the plots are shown for the range from 5 kHz to 20 kHz. The nine coefficient sets are compared to each other for each fleece separately. It can be observed, that all coefficient sets except of Komatsu yield very similar results. This is surprising, as most of them are far beyond their validity range. The very different performance of the Komatsu fitting is caused by its very different coefficients (see table 2.8). It is the only coefficient set that includes negative coefficients.

fitting	applicability	valid freq. range
Delany-Bazley	glass and rock wool $0.01 \leq X \leq 1$ $10^3 \leq R_f \leq 50 \cdot 10^3 \text{ Pa}\cdot\text{s}/\text{m}^2$	—
Miki	glass and rock wool $0.01 \leq X \leq 1$ $10^3 \leq R_f \leq 50 \cdot 10^3 \text{ Pa}\cdot\text{s}/\text{m}^2$	—
Qunli	porous plastic and open foams $200 \leq f \leq 2000 \text{ Hz}$ $3 \cdot 10^3 \leq R_f \leq 24 \cdot 10^3 \text{ Pa}\cdot\text{s}/\text{m}^2$	—
Mechel, glass fiber, low X	glass fiber $X \leq 0.025$	$f \leq 17.5 \text{ kHz}$
Mechel, glass fiber, high X	glass fiber $X \geq 0.025$	$f \geq 108.3 \text{ kHz}$
Mechel, rock fiber, low X	rock fiber $X \leq 0.025$	$f \leq 17.5 \text{ kHz}$
Mechel, rock fiber, high X	rock fiber $X \geq 0.025$	$f \geq 108.3 \text{ kHz}$
Komatsu	glass and rock wool $6 \cdot 10^3 \leq R_f \leq 73 \cdot 10^3 \text{ Pa}\cdot\text{s}/\text{m}^2$	—
Modified Champoux and Allard	$45 \text{ Hz} \leq f \leq 11 \text{ kHz}$	$45 \text{ Hz} \leq f \leq 11 \text{ kHz}$

Table 2.12: validity of the different fittings for the Delany-Bazley model according to [3, p. 272]

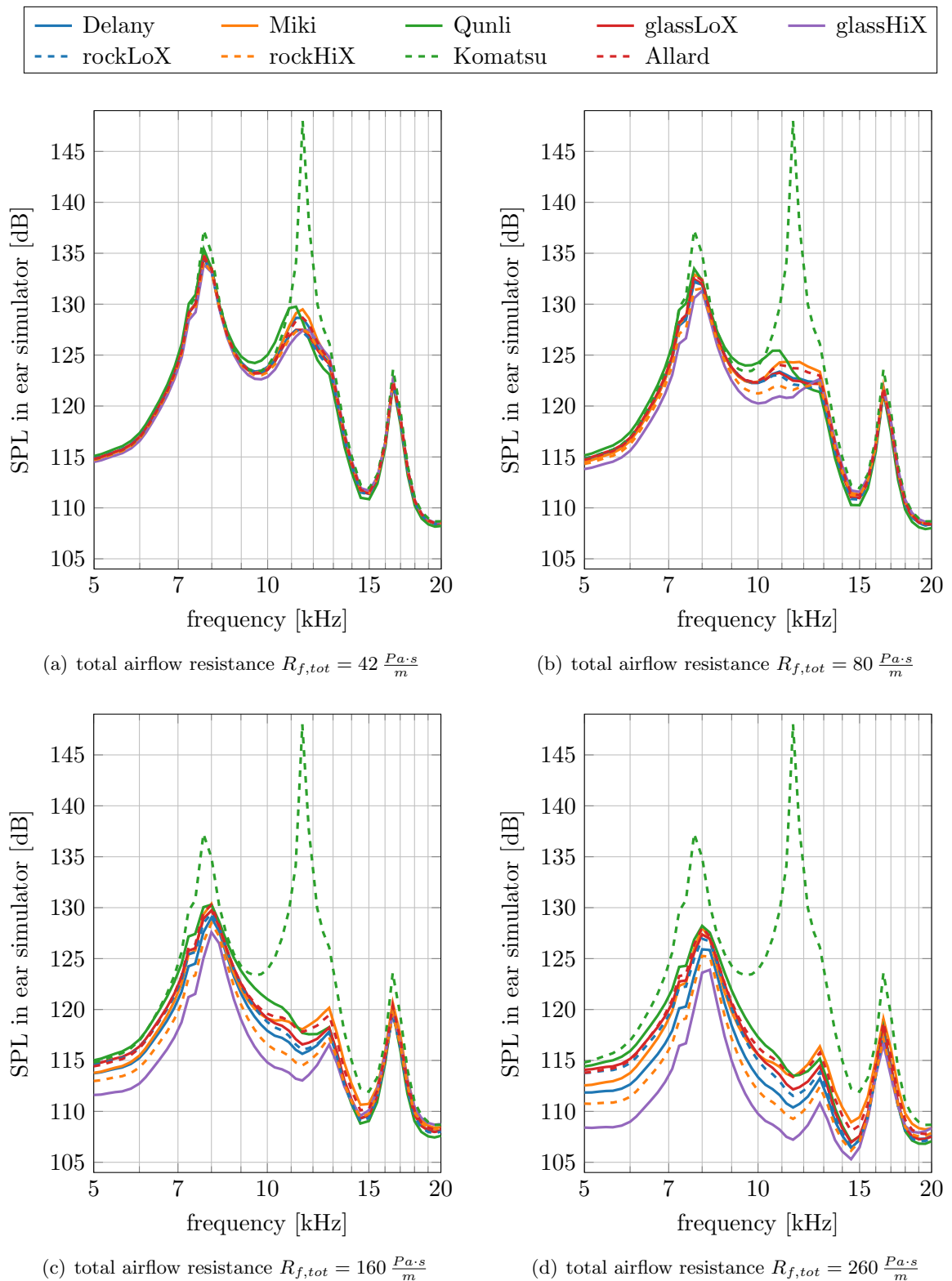


Figure 2.10: comparison of the different coefficient sets for the Delany-Bazley model in Comsol for different acoustic fleeces

2.4 Ear Simulator Model

An ear simulator is a standardized device to imitate the acoustic behaviour of an average human ear. It is specified in the international standard IEC 60318-4. Even though the acoustic response of the ear simulator is only specified up to 10 kHz by the standard, the device is typically used up to 20 kHz as the whole human audible frequency range has to be investigated.

The ear simulator consists of a cylindrical air volume that is terminated with a microphone membrane. Two resonators ($f_{res,1} \approx 1 \text{ kHz}$, $f_{res,2} \approx 3.5 \text{ kHz}$, see [12]) are connected to this cylinder in order to reproduce the human ear's frequency response. For the measurements in this work, a GRAS RA0045 ear simulator is used (see figure 2.11(a)). A model of the ear simulator already exists in the Cansol library [12]. It is originally designed to match the ear simulator from Brüel & Kjær. As the acoustic performance of the ear simulator is specified in detail by the standard, the devices from these two manufacturers are interchangeable. Thus, the existing model is used for this work. It is shown in figure 2.11(b).

The model of the ear simulator is briefly summarized here. For more information it is referred to the Cansol documentation [12]. The enclosed air volume inside the ear simulator is modelled as a lossless pressure acoustics domain. Only in the narrow slits losses are considered using the narrow region acoustics feature. The microphone is modelled with an impedance boundary condition based on an equivalent RLC network. All other boundaries are modelled as sound hard walls.

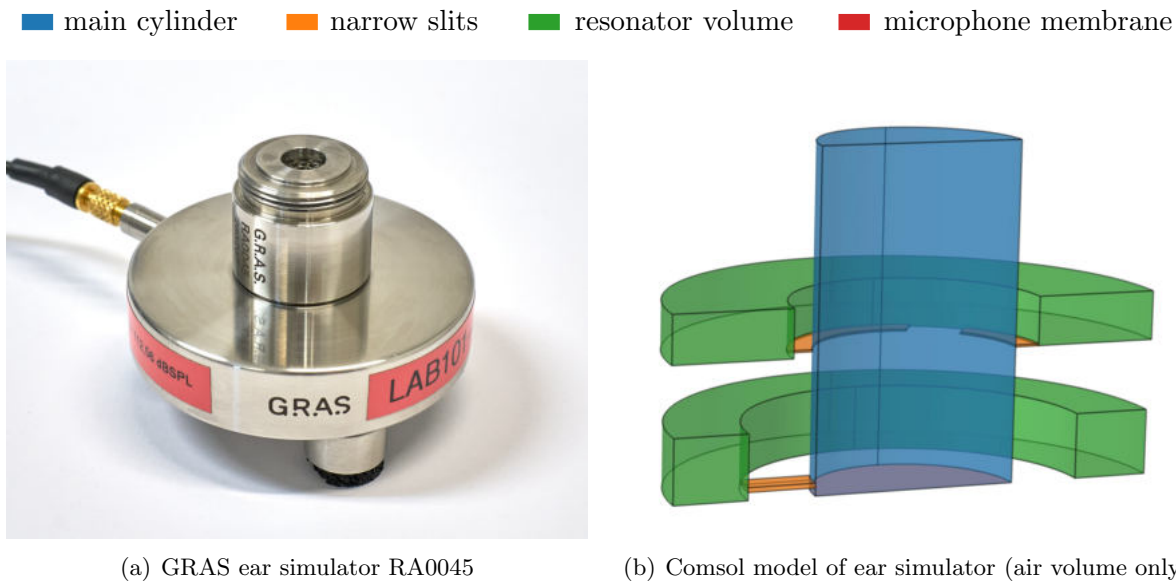


Figure 2.11: standardized ear simulator to imitate the human ear canal

The model of the ear simulator is used in this work in two different ways. On the one hand, it is fully imported into the Cansol project and connected to the headphone-adaptor model. On the other hand, it is used to calculate the input impedance and the transfer function of the ear simulator in order to reduce the model's complexity. The calculation of these quantities is described in section 2.4.1. Section 2.4.2 shows how the derived quantities are used to set up a simplified impedance model. The impedance model and the full model are compared to each other and show perfect agreement.

2.4.1 input impedance and transfer function

The input impedance of the ear simulator is defined as the ratio of the average acoustic pressure p and the average normal velocity at the input surface of the ear simulator. The normal velocity is the velocity component in the direction of the normal vector of the input surface pointing into the ear simulator. In the model, this is the negative z direction. The z component of the velocity is denoted in Comsol by the variable $acpr.vz$.

In order to obtain the averaged values of pressure and velocity, the averaging function $\text{avg_in}()$ is defined on the input surface of the ear simulator. It returns the average value of its input argument on the defined input surface of the ear simulator. With these quantities, the input impedance of the ear simulator is defined as a new variable Z_{in} inside the Comsol model of the ear simulator according to equation 2.19.

$$Z_{in} = \frac{\text{avg_in}(p)}{\text{avg_in}(-acpr.vz)} \quad (2.19)$$

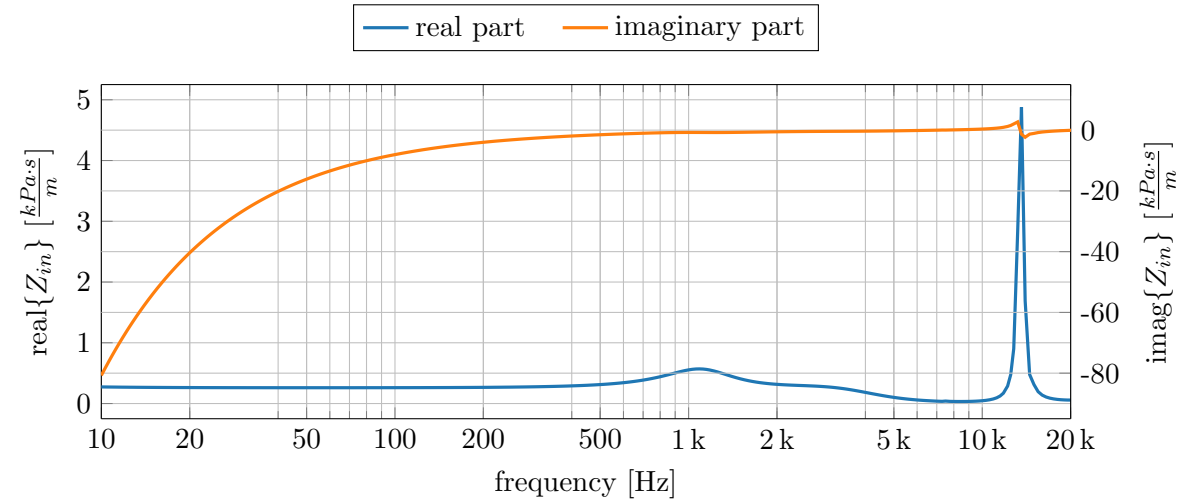
The transfer function of the ear simulator is defined as the ratio of the average acoustic pressure at the microphone and the average acoustic pressure at the input surface. Hence, another averaging function $\text{avg_mic}()$ is defined on the surface of the microphone membrane. The value of the transfer function is stored in a new variable H_{ear} . It is calculated according to equation 2.20.

$$H_{ear} = \frac{\text{avg_mic}(p)}{\text{avg_in}(p)} \quad (2.20)$$

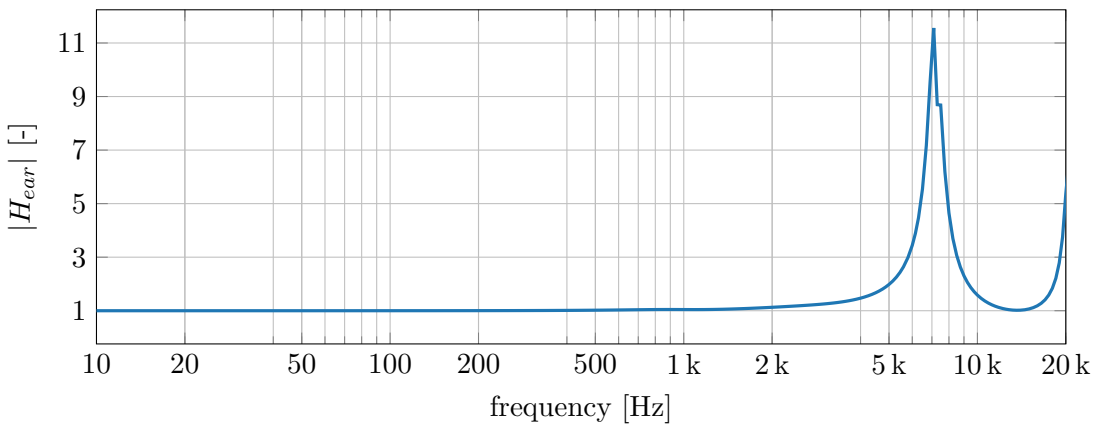
In order to evaluate these quantities, the pressure distribution inside the ear simulator has to be calculated. For this reason, a normal velocity boundary condition is defined at the input area of the ear simulator to excite the model. As the whole model is linear, the value of this input velocity does not affect the calculated input impedance and transfer function of the system. It is arbitrarily set to an amplitude of 0.1 m/s ($L_v = 123 \text{ dB}$, $v_{eff} = 0.07 \text{ m/s}$, $v_0 = 5 \cdot 10^{-8} \text{ m/s}$). The model is solved for the frequencies from 10 Hz to 20 kHz with a resolution of $1/24$ octave.

In order to use the calculated quantities in the adapter model, the values are exported and saved in a text file. This file can then be imported into the Comsol project of the adapter model and used to define an impedance boundary condition (see section 2.4.2). Since interpolation between complex values is not possible in Comsol, the real and imaginary parts of the calculated input impedance are exported separately. The phase information of the transfer function is not needed in the adapter model, as only the SPL at the microphone is investigated. Therefore, only the magnitude of the transfer function is exported.

The exported quantities are plotted in figure 2.12. At approximately 7 kHz the height of the ear simulator corresponds to a quarter of the acoustic wave length. Hence, the sound pressure at the input surface of the ear simulator becomes very low due to destructive interference yielding a maximum of the transfer function H_{ear} (see figure 2.12(b)). At approximately 14 kHz the height of the ear simulator corresponds to half of the acoustic wave length. Thus, constructive interference at the input surface of the ear simulator leads to a maximum of the sound pressure and therefore to a maximum of the input impedance Z_{in} (see figure 2.12(a)).



(a) calculated input impedance of the ear simulator



(b) magnitude of the calculated transfer function of the ear simulator

Figure 2.12: calculated input impedance and transfer function of the ear simulator derived from the Cansol model

2.4.2 impedance model vs. full model

The full model is obtained by combining the headphone model, the adapter model and the ear simulator model in one Cansol project. The SPL at the microphone inside the ear simulator can then directly be accessed in the calculated solution. The ear simulator remains always unchanged in the model while the headphone geometry, the acoustic fleece, the insertion depth and the venting hole are changing. It therefore makes sense to replace the ear simulator by its input impedance in order to reduce the model's complexity. The SPL at the microphone is then obtained with the help of the transfer function of the ear simulator. Both, the full model and the resulting impedance model are shown in figure 2.13. Since the symmetry of the model is exploited, only half of the geometry is shown.

The calculated input impedance and transfer function data (see section 2.4.1) are integrated into linear interpolation functions in the adapter model. The data is saved in text files with a resolution of $1/24$ octave. These text files are imported into the corresponding interpolation functions and saved there as a local table in the Cansol project. Three interpolation functions are needed for the real part of the input impedance, the imaginary part of the input impedance and the magnitude of the transfer function. They are listed in table 2.13. Direct interpolation of complex numbers is not possible in Cansol.

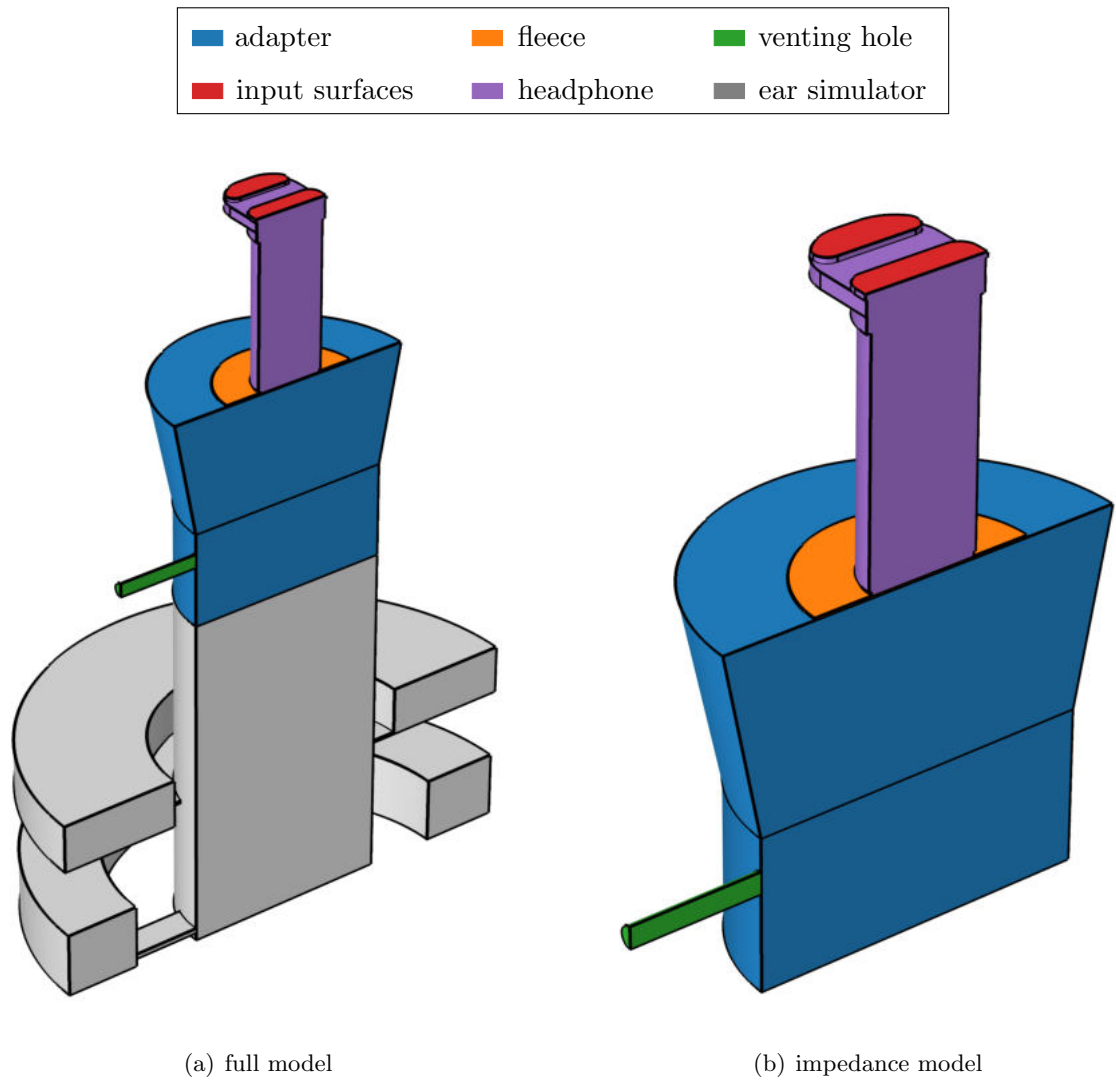


Figure 2.13: the full model of the ear simulator is replaced by an impedance boundary condition

The simulations in this work are conducted with the same resolution ($1/24$ octave) as the calculation of the impedance data. Therefore, the interpolation functions are only evaluated at the data points and no interpolation is done. However, with this implementation, the user can evaluate the impedance and transfer function - and thus the simulation - at any frequency in the range 10 Hz to 20 kHz.

interpolation function	description
<code>Zin_ear_re</code>	real part of the input impedance of the ear simulator
<code>Zin_ear_im</code>	imaginary part of the input impedance of the ear simulator
<code>H_ear_abs</code>	magnitude of the transfer function of the ear simulator

Table 2.13: user defined linear interpolation functions in the adapter model with the imported input impedance and transfer function data from the ear simulator model

With the interpolated impedance data, an impedance boundary condition is defined on the bottom surface of the adapter. It is described by equation 2.21. The impedance Z_i is entered

as an user defined impedance model according to equation 2.22. The $freq$ variable holds the studied frequencies of the simulation.

$$\mathbf{n} \cdot \frac{\nabla p}{\rho_c} = -\frac{i\omega p}{Z_i} \quad (2.21)$$

$$Z_i = Z_{in_ear_re}(freq) + i \cdot Z_{in_ear_im}(freq) \quad (2.22)$$

The impedance boundary condition is only valid if the waves propagate in the boundary's normal direction \mathbf{n} . For the studied frequency range the minimum wavelength is 1.7 cm at 20 kHz, which is much larger than the diameter of the main cylinder of the ear simulator (3.5 mm). It is therefore a valid assumption that there is no wave propagation in the radial direction of the main cylinder of the ear simulator.

With the impedance model, the sound pressure at the microphone in the ear simulator is not directly available in the solution. It is obtained by multiplying the sound pressure at the outlet of the adapter with the imported transfer function of the ear simulator. A new variable $p_{avg,mic}$ is defined according to equation 2.23. It contains the averaged effective sound pressure at the microphone in Pa. $H_{ear_abs}(freq)$ denotes the interpolated magnitude of the transfer function of the ear simulator evaluated at the studied frequency. The averaging function $avg_out()$ is defined on the outlet surface of the adapter. $acpr.p.t_rms$ is a Cmsol internal variable holding the effective value of the calculated sound pressure.

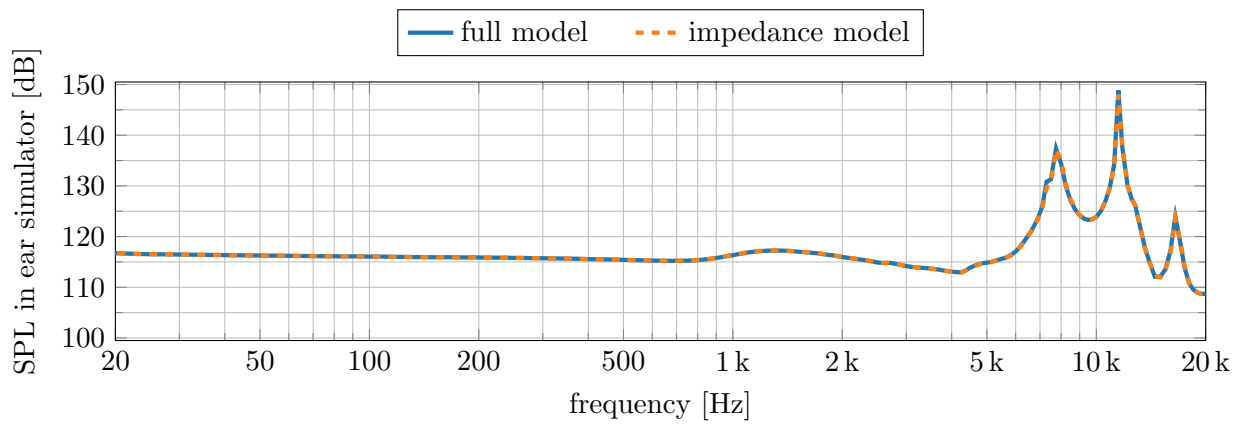
$$p_{avg,mic} = avg_out(acpr.p.t_rms) \cdot H_{ear_abs}(freq) \quad (2.23)$$

Note: Since the amplitude of the calculated sound pressure is complex valued, there are generally two ways to calculate an average effective value over the microphone area. On the one hand, the complex amplitudes of the sound pressure can be averaged for all discrete points on the microphone membrane, and then the effective value of this average is determined. On the other hand, the effective sound pressure can be calculated for each point on the membrane, and then the average of these effective values is determined. In general, these two approaches yield different results. With the assumption that there is no wave propagation in the radial direction of the membrane, the complex amplitudes of the sound pressure at the microphone must all have the same phase. In this particular case, both approaches are identical. In equation 2.23 the second approach is implemented.

The calculated sound pressure is then used to obtain the sound pressure level at the microphone according to equation 2.24. The value is stored in the variable SPL_{mic} .

$$SPL_{mic} = 20 \cdot \log_{10} \left(\frac{p_{avg,mic}}{20 \mu Pa} \right) \quad (2.24)$$

Figure 2.14 shows the calculated SPL at the microphone for the full model and the impedance model. The results are compared exemplary for three model configurations. A perfect match of the two models is clearly visible. The impedance model is therefore used for the simulations in this work.



(a) no fleece, no venting, 5 mm insertion depth

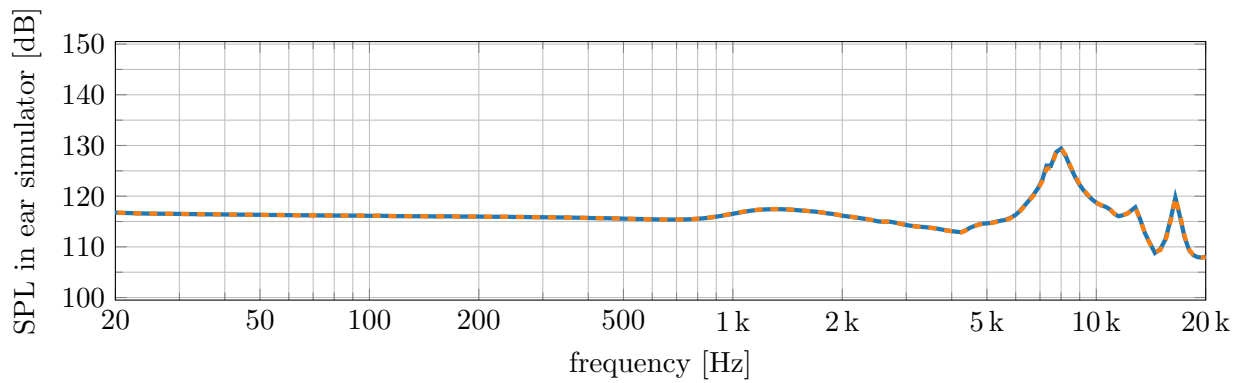
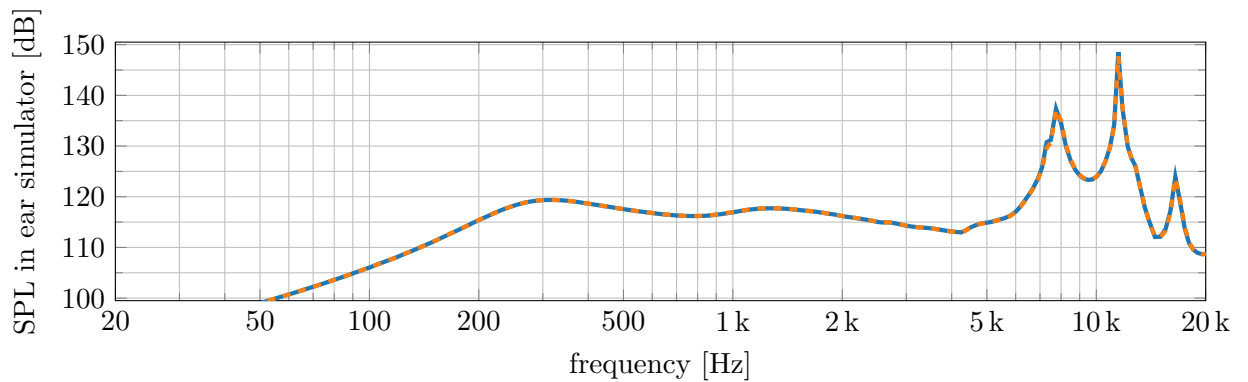
(b) $R_{f,tot} = 160 \text{ Pa}\cdot\text{s}/\text{m}$ fleece, no venting, 5 mm insertion depth(c) no fleece, $\varnothing 0.5 \text{ mm}$ hole, 5 mm insertion depth

Figure 2.14: comparison of the full model and the impedance model for different configurations

3

Measurements and Validation

The following chapter describes the measurements that have been done to ensure valid model inputs and outputs. In section 3.1 the measurement of the loudspeaker membrane velocity is shown. Ten speakers are measured with a laser Doppler vibrometer. The averaged velocity is used as an input for the normal velocity boundary condition in the Cmsol model.

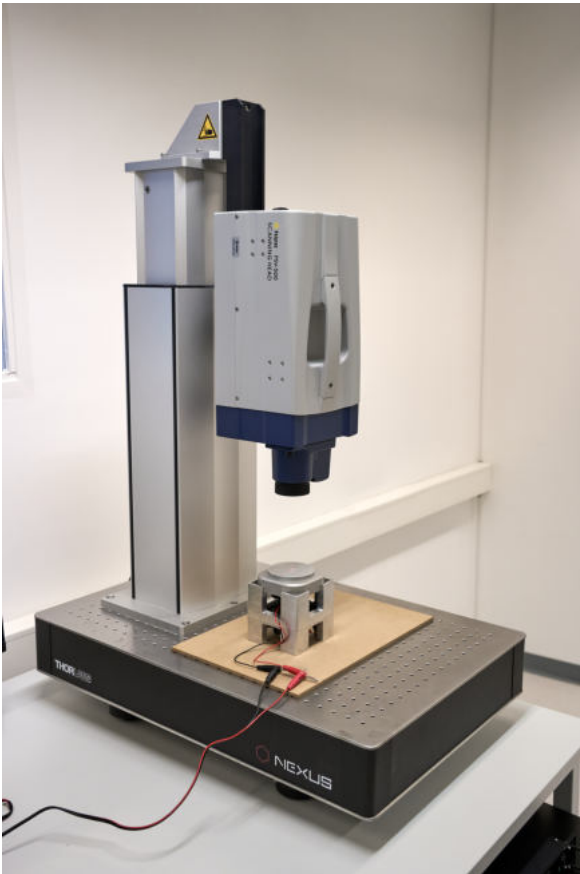
In section 3.2 the measurements of the headphone prototypes in a standardized GRAS ear simulator are discussed. The measured sound pressure level (SPL) is compared to the calculated results from the Cmsol model. Several parameters like the insertion depth of the headphone, the size of the venting hole and the properties of the acoustic fleece are varied in the simulation as well as in the measurements to obtain a good validation of the model.

3.1 Membrane Velocity

The average membrane velocity of the Achelous loudspeaker is needed to define a source condition in the Cmsol model. The source is modelled with the *normal velocity* boundary condition inside the pressure acoustics domain, thus assuming a plane movement normal to the boundary. As the loudspeaker membrane is fixed on the edges, the assumption of a plane movement of the whole membrane is not true. To keep the model simple, an empirical value for the effective membrane area has been used, which is smaller than the real membrane area. It corresponds to a planar moving surface with the velocity at the membrane centre-point, that produces the same volume velocity as the real membrane. Therefore only the centre-point of the membrane is measured in this work.

The measurements have been done with a Polytec PSV-500 laser Doppler vibrometer (see figure 3.1(a)). The output signal for the loudspeaker is generated by the Polytec front end (see figure 3.1(b)). The studied loudspeaker is based on the deformation of a piezoelectric material and requires a DC offset of the input signal. It should be driven by a sinusoidal signal with an amplitude of 15 V and a 15 V DC offset. As the front end is limited to a maximum of 10 V output voltage, an additional amplifier is used to achieve the desired amplitude. The amplified signal is fed to the loudspeaker.

The speaker has been mounted on the laser Doppler vibrometer with a special made adapter. The adapter contains an opening that allows to mount and contact the speaker without covering the front opening of the membrane. In the measurement setup the speaker's surface is pointing upwards and the laser is pointing to the center of the membrane from above. Figure 3.2(a) shows the bottom side of the Achelous speaker in the measurement adapter. The speaker is contacted with a matching plate on the adapter (see figure 3.2(b)). The plate contains two banana connectors, that are connected to the signal generator output of the Polytec front end.



(a) laser Doppler vibrometer

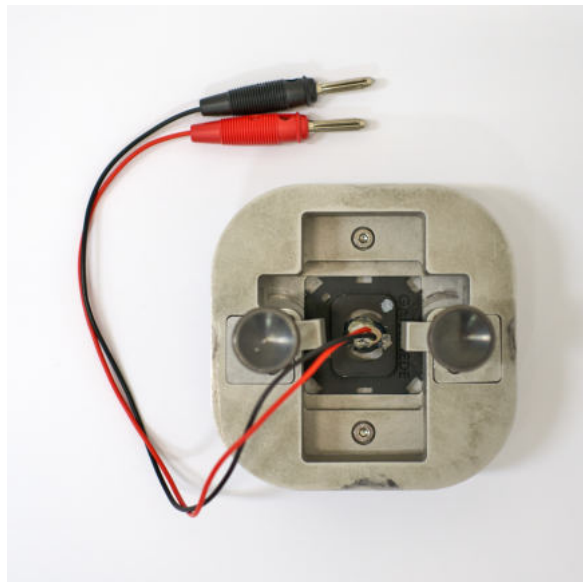


(b) computer, front end and amplifier used for the measurement

Figure 3.1: vibrometer and measurement hardware



(a) Achelous speaker inside special made adapter (bottom view)



(b) speaker connected with connection plate

Figure 3.2: loudspeaker measurement adapter

The distance between the laser head and the speaker membrane is approximately 23 cm. Before starting the measurement, the laser has to be focused on the membrane and aligned with the camera picture on the computer screen. Figure 3.3(a) shows the mounted speaker in the measurement adapter from above. The measurement point is defined on the center of the membrane in the Polytec software (see figure 3.3(b)).

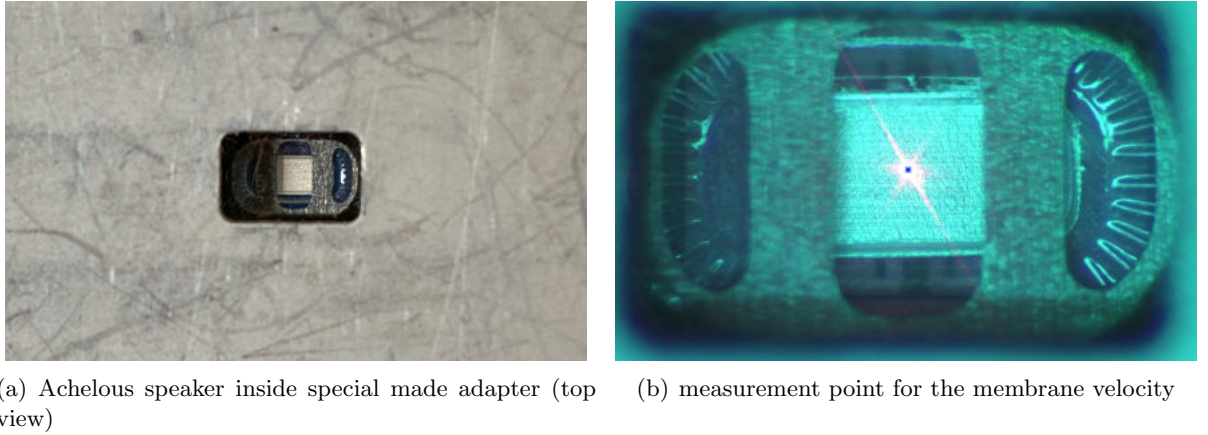


Figure 3.3: mounted Achelous speaker

The measurement has been repeated with ten Achelous loudspeakers with stepped sine signals in the range from 20 Hz to 20 kHz. The step size has been set to a semitone ($f_{n+1}/f_n = \sqrt[12]{2} \approx 1.06$) yielding 121 data points. Figure 3.4 shows the measured peak value of the membrane velocity for the ten different speakers and their average. The averaged velocity amplitude v_{peak} has been used as an input for the Comsol simulation. For studying the low frequency behaviour of the venting hole, the velocity data has been manually extrapolated downwards to 10 Hz, following the decay in amplitude by a factor of two per frequency octave towards low frequencies.

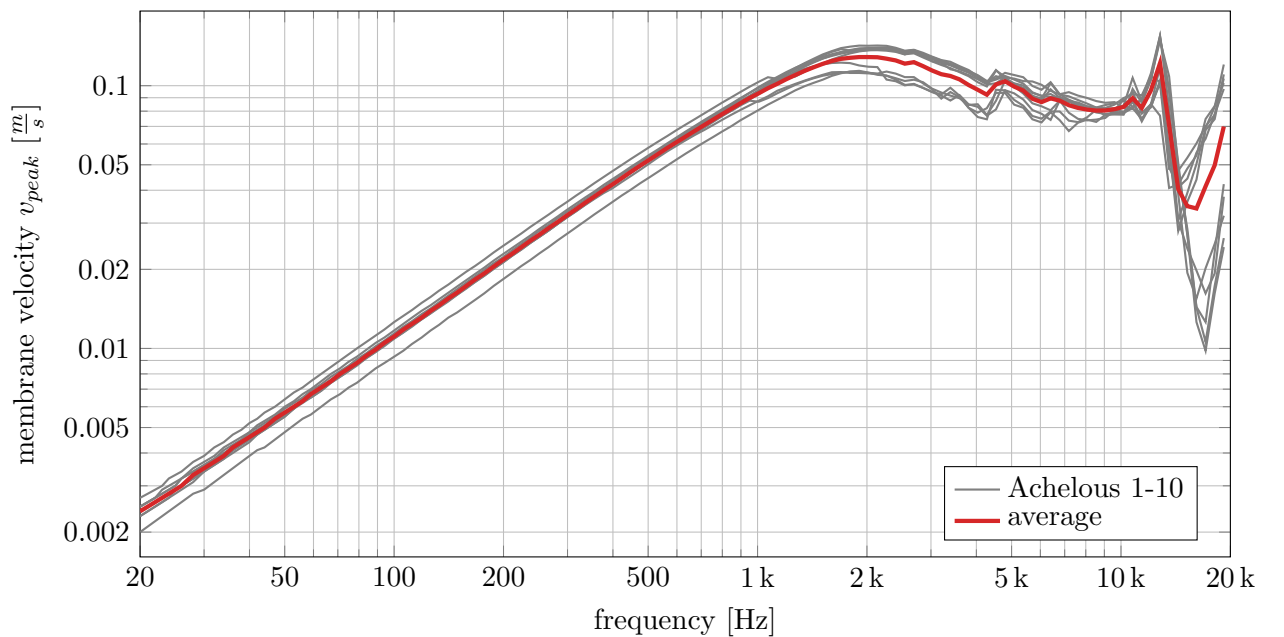


Figure 3.4: measured membrane velocity amplitude for ten different Achelous speakers

3.2 SPL inside the Ear Simulator

To validate the Comsol model five headphone prototypes have been built. The prototypes consist of Achelous speakers glued into the front shell of the headphones with a sealing tape (see figure 3.5(a)). The geometry of the used front shells equals the geometry of the headphone file imported into the Comsol model.

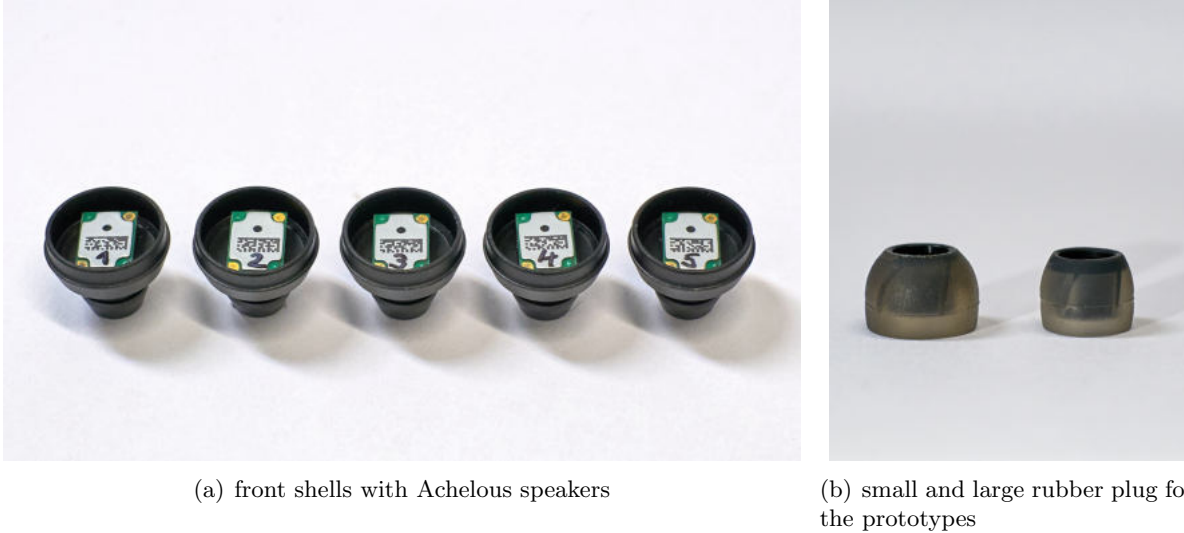


Figure 3.5: headphone prototypes

The prototypes have been measured in a standardized GRAS ear simulator to imitate the behaviour inside the human ear. The used equipment and setup is described in the next section. Several modifications have been investigated in the measurements and simulations. All modifications have been applied equally to all of the five prototypes. By comparing the results the model was validated and improved.

Section 3.2.2 shows, that variations of the insertion depth of the headphone into the ear simulator are covered well by the model. The performance of different coefficient sets of the poroacoustic Delany-Bazley submodel for the acoustic fleece is discussed in section 3.2.4. Using fleeces with an airflow resistance in the range from $42 \text{ Pa}\cdot\text{s}/\text{m}$ to $260 \text{ Pa}\cdot\text{s}/\text{m}$ the best matching coefficient set is chosen for the model.

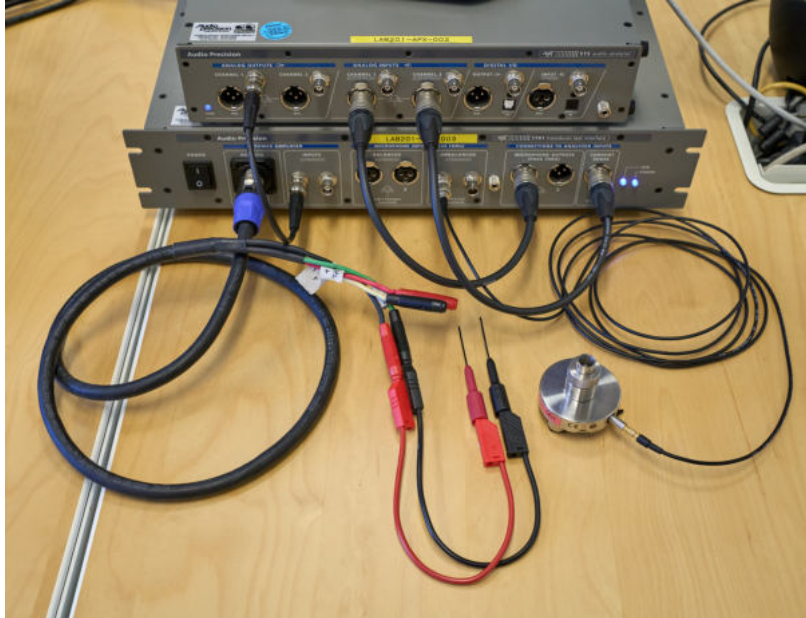
The venting hole is modelled with the narrow region feature inside the pressure acoustics domain and terminated with an open pipe impedance boundary condition in Comsol. It shows a good performance for larger diameters, but poor alignment with the measurements for the smallest hole. This leads to an empirical adjustment rule of the model depending on the venting diameter, which is elaborated in section 3.2.3.

3.2.1 equipment and setup

The measurements have been done with a GRAS RA0045 ear simulator, which is designed to imitate the human ear. It contains resonance absorbers to account for losses in the human ear and approximates the acoustic behaviour of an average human ear canal. Its frequency response is standardized by IEC 60318-4 up to 10 kHz, but it is usually used for the whole human audible frequency range (20 Hz - 20 kHz). The ear simulator and its Comsol model are described in more

detail in section 2.4.

The ear simulator signal is passed through an Audio Precision APx 1701 transducer test interface and fed into the analog input of an Audio Precision APx 515 audio analyzer. It is sampled with a frequency of 96 kHz. The output signal for the speaker is generated by the APx 515 and amplified by the APx 1701. The headphone prototypes are connected to the ear simulator with an in-ear adapter and contacted manually during the measurements with test prods. The setup is shown in figure 3.6.



(a) Audio Precision hardware with GRAS ear simulator



(b) contacted headphone in in-ear adapter on the ear simulator

Figure 3.6: setup for the ear simulator measurements

Two different in-ear adapters have been used for the measurements. The regular GRAS RA0088 adapter was used for investigations of the insertion depth and the acoustic fleece. A special made leakage adapter, which contains four different venting holes, has been used for the venting studies. The adapters are described in section 2.3. The used hardware is listed in table 3.1.

part	description
headphone prototypes	USound Achelous speaker + front shell
ear simulator	GRAS RA0045 ear simulator
in-ear adapter	GRAS RA0088
leakage adapter	special made (four holes)
signal analyzer	Audio Precision APx 515 audio analyzer
test interface	Audio Precision APx 1701 transducer test interface

Table 3.1: equipment used for the SPL measurements

For all measurements a sinusoidal sweep from 10 Hz to 20 kHz has been used. The signal amplitude has been set to 15 V. A superimposed 15 V DC offset was necessary due to the piezoelectric

actuator inside the speaker. This is the same amplitude that has been used for the measurement of the membrane velocity (see section 3.1), and therefore as an input for the Comsol model.

In addition to the ear simulator signal, the current through the amplified output channel is measured and fed into the second input channel of the audio analyzer. The APx 1701 offers a so called *current sense* output to do this. The current signal allows for calculation of the speaker's impedance, which can be used to identify mechanical damage of the speaker. The impedance was only used for monitoring the speakers' condition during the measurements and is not discussed further in this work.

3.2.2 variation of insertion depth

The insertion depth of the headphone inside the ear simulator may vary for different headphone geometries and earplug sizes. Therefore a variable h_{insert} was created in the Comsol model (see section 2.1) to modify the height of the resulting air cone inside of the adapter. It is important to verify that the Comsol model is able to represent the effect of these variations on the measured SPL properly. Thus, in this section the measured SPL is compared to the simulated results.

The insertion depth of the prototypes inside the GRAS in-ear adapter has been adjusted to the values 4 mm, 5 mm, 6 mm and 7 mm. The 7 mm were achieved using the small rubber plug, for the other depths the larger rubber plug was used (see figure 3.5(b)). The Comsol model has been modified accordingly. The headphone setup and the Comsol model are exemplary shown for the values $h_{insert} = 5\text{ mm}$ and $h_{insert} = 7\text{ mm}$ in figure 3.7. For studying the effect of the different insertion depths no venting hole and no acoustic fleece has been used.

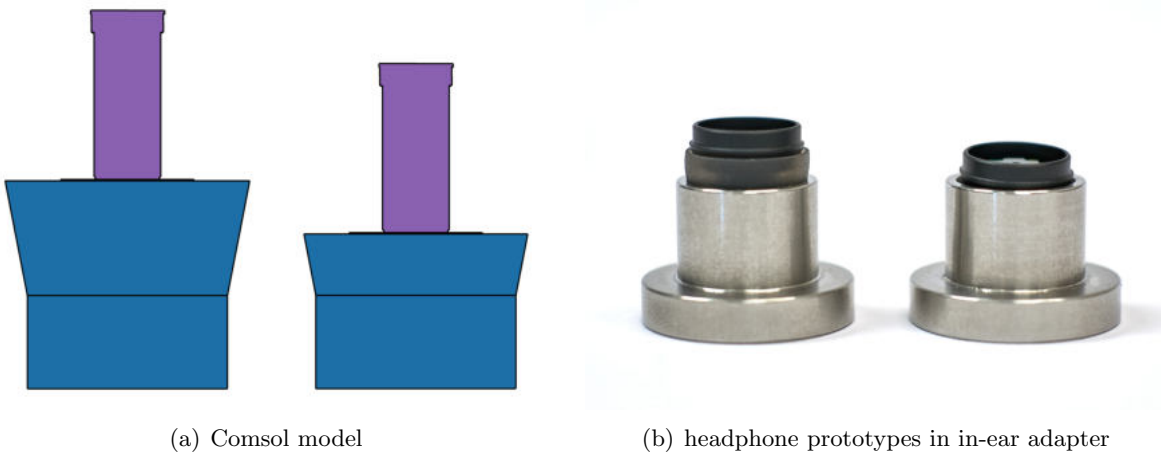


Figure 3.7: Comsol model and headphone setup for insertion depths of 5 mm (left) and 7 mm (right)

All of the five prototypes have been measured in the four different configurations of h_{insert} . Figure 3.8 compares the results to the Comsol simulation. The match of measurement and simulation is very good. The location of the resonance peaks is predicted very well by the model. Only the amplitude at the resonances is overestimated. This can be explained by the fact, that the Comsol model is almost completely lossless (without the acoustic fleece and the venting hole). Only in the narrow slits inside the ear simulator thermoviscous boundary losses are considered.

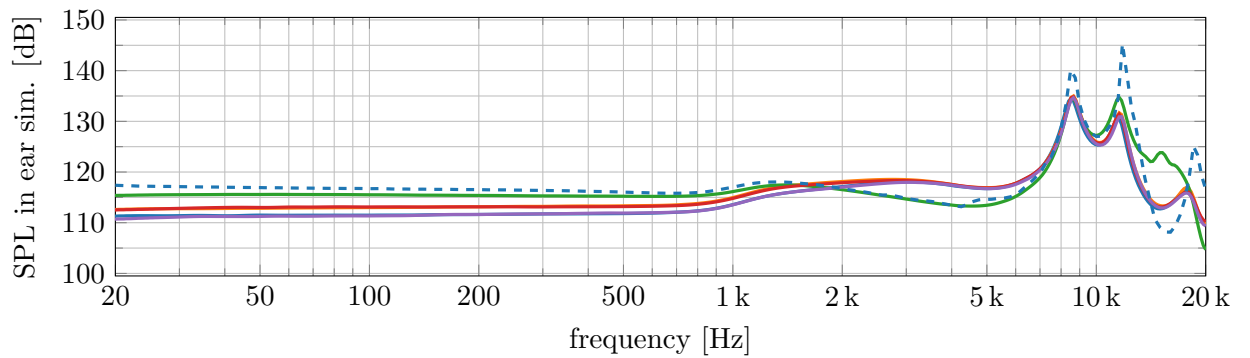
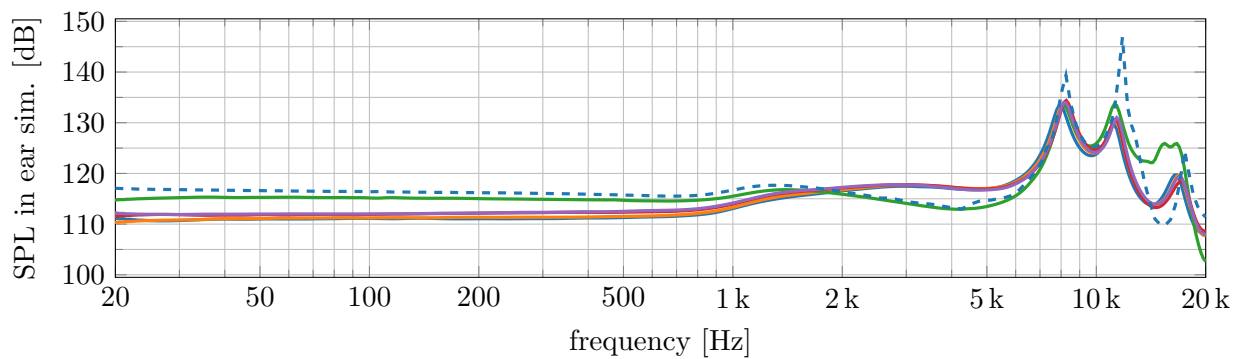
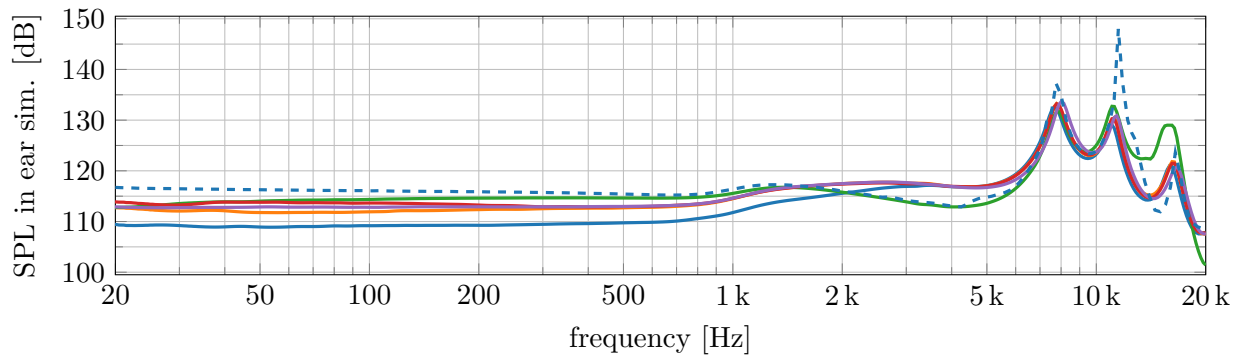
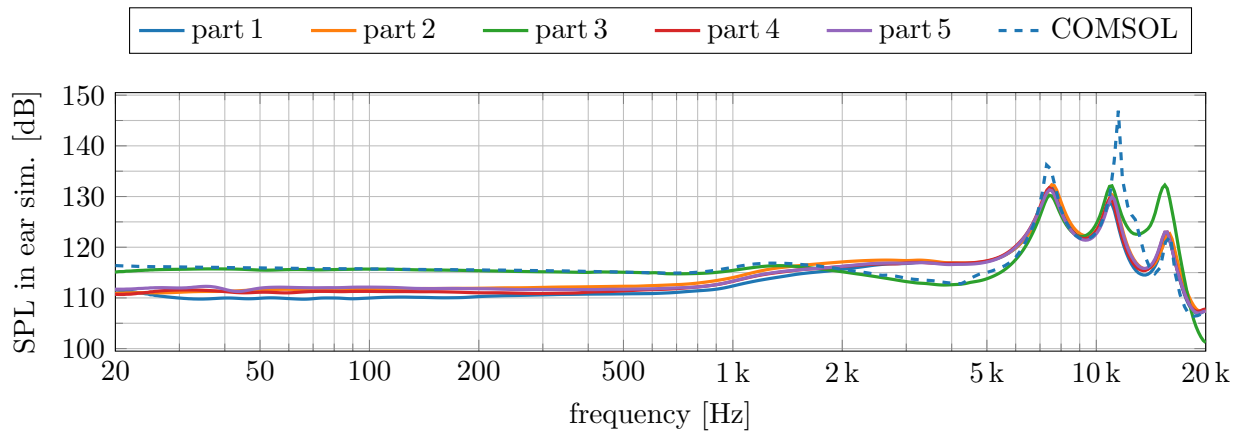
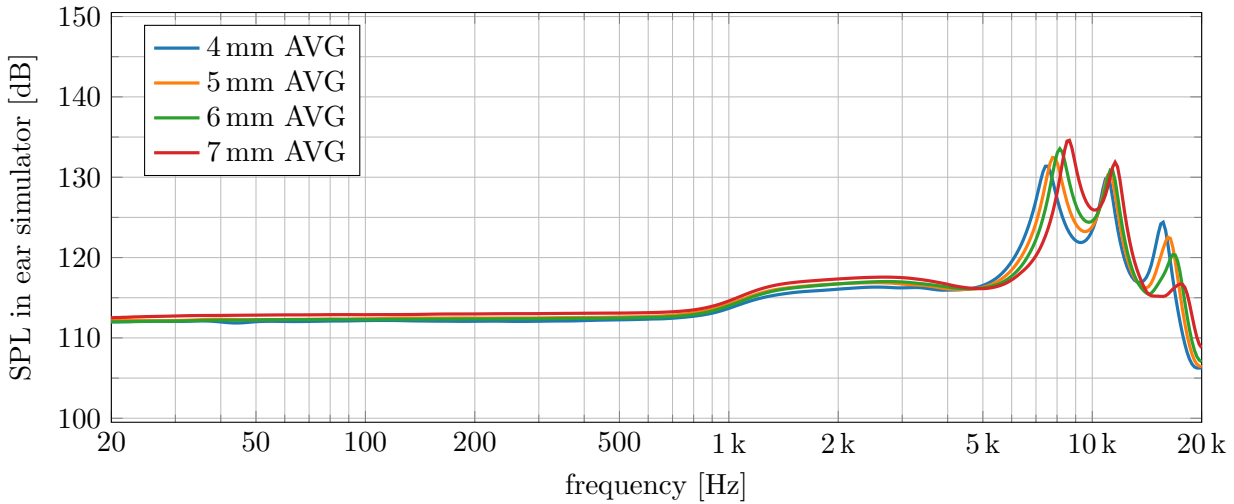


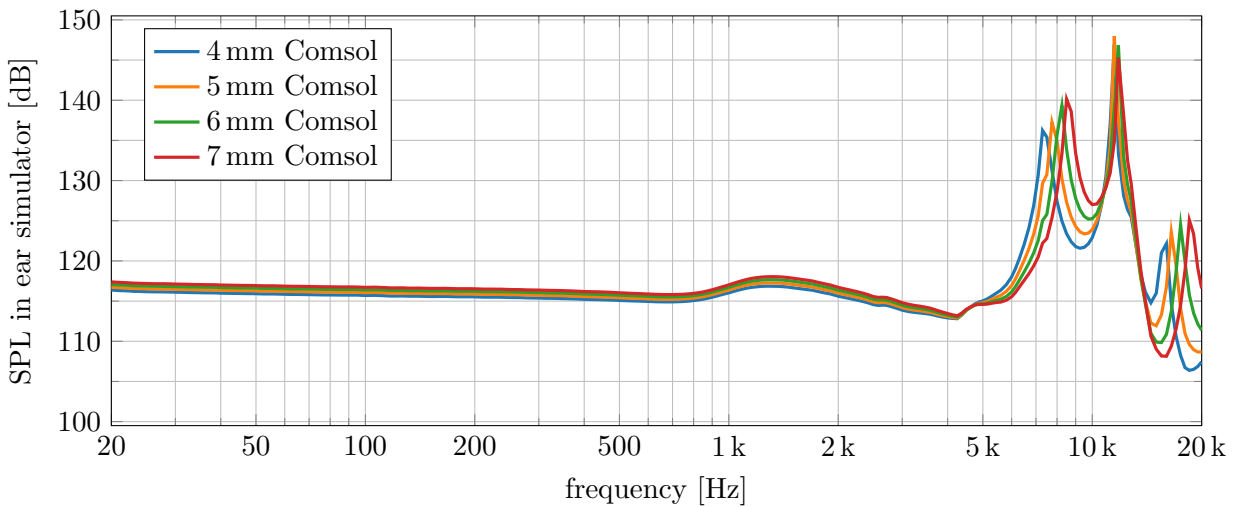
Figure 3.8: measurement results of the five headphone prototypes compared to the Comsol model for different insertion depths

In order to compare the different configurations of h_{insert} with each other, the five prototypes are averaged for each insertion depth. The results are shown in figure 3.9(a). It can be observed, that the first and the third resonance peak at approximately 8 kHz and 16 kHz are shifted towards higher frequencies when the headphone is pushed further inside the ear simulator. These peaks are caused by the $\lambda/2$ and λ resonance inside the combined air volume of the main cylinder of the ear simulator and the attached adapter. Pushing the headphone further inside the adapter shortens the length of the enclosed air volume and therefore shifts these resonances. The second peak at approximately 11.5 kHz however, is caused by a $\lambda/4$ resonance inside the headphone. Its resonance frequency is therefore almost independent of the insertion depth.

Figure 3.9(b) shows the same comparison for the simulated results. The plots show the same behaviour like the measurements: increasing the insertion depth leads to a shift of the first and third peak towards higher frequencies while the second peak is almost independent of the insertion depth. As already discussed in figure 3.8, the amplitude at the resonances is too high in the simulation. Apart from that, the model works very well to predict the SPL inside the ear simulator for different insertion depths.



(a) measurement: average over the five prototypes



(b) Comsol simulation

Figure 3.9: measurement averages and simulation for different insertion depths of the headphone

The value $h_{insert} = 5\text{ mm}$ seemed most suitable for the prototypes without pressing them into the ear simulator too hard or being too loose. Therefore, this value has been chosen as a reference and was used for the studies of venting and fleece variations.

3.2.3 variation of venting

Using a venting hole inside an in-ear headphone allows for static pressure compensation between the ear canal and the ambient air. This improves the wearing comfort and ensures that the speaker's membrane can move freely without an offset. However, using a venting hole is like applying a high pass filter to the SPL inside the ear (simulator). Therefore, it is very important to design the venting properly in order to not cut relevant frequencies of the desired audio signal. The created Comsol model helps to reduce the time and money consuming prototyping phase in order to optimize the venting size. The model of the venting hole is described in section 2.3.1. The losses inside the narrow hole are modelled with the *Narrow Region* feature and the open end is modelled with a suitable impedance boundary condition.

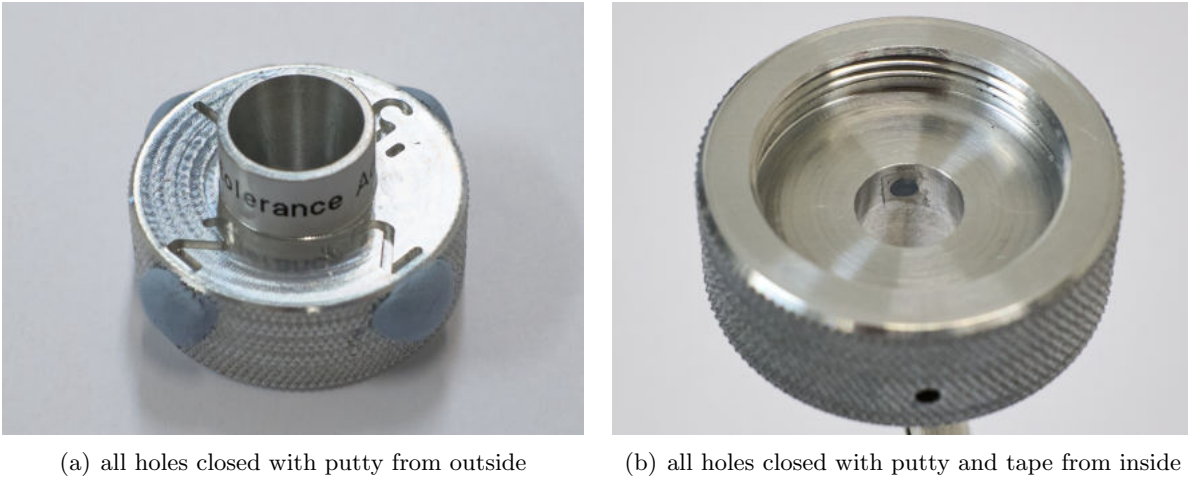
In this section the validation of the venting model is described. Measurements have been done with four different venting diameters: $\varnothing 0.2\text{ mm}$, $\varnothing 0.5\text{ mm}$, $\varnothing 1\text{ mm}$ and $\varnothing 2\text{ mm}$. By comparing the simulated results with the measurements, an empirical adjustment factor is elaborated, to improve the model's performance for very narrow venting holes. In order to not destroy the headphone prototypes for the measurements, a special made leakage adapter has been used on the ear simulator. Its inside air volume is identical to the one of the standard GRAS in-ear adapter, but it contains four different holes. For more information about the leakage adapter and its geometry see section 2.3.

In the final design, the venting hole has to be included in the headphone of course. A shift of the hole by a few millimetres from the headphone to the adapter is acoustically negligible, as the hole is only relevant at low frequencies where the wavelength is several meters. This simplification can therefore be accepted here. In the simulations the hole has been modelled at the same location inside the adapter.

All measurements in this section have been done with the insertion depth $h_{insert} = 5\text{ mm}$ of the headphones inside the leakage adapter and without any acoustic fleece. The displayed measurement curves are the average of five measurements using the same setup with each of the five prototypes.

To ensure a good comparability of the venting studies in the leakage adapter with the reference measurement in the standard adapter, the two adapters have been compared with each other, while all holes of the leakage adapter are closed. The holes can easily be closed from outside with putty (see figure 3.10(a)). Using this method, the venting holes stay connected to the main volume of the adapter and behave as a closed pipe resonator influencing the result. Therefore, the more laborious method of closing the holes from the inside of the adapter has to be chosen (see figure 3.10(b)). The putty has been squeezed into the holes with tweezers from inside. To ensure a plane surface on the inside, the closed holes have been covered with a small piece of tape.

Figure 3.11 shows the measured SPL inside the ear simulator for the two different methods of closing the holes of the leakage adapter. The results are compared to the averaged reference measurement in the standard adapter. Closing the holes from inside yields almost perfect agreement with the standard adapter. Only a small deviation around 14 kHz can be observed, which might be caused by the not perfectly rigid closure of the holes.



(a) all holes closed with putty from outside

(b) all holes closed with putty and tape from inside

Figure 3.10: closing the holes of the leakage adapter

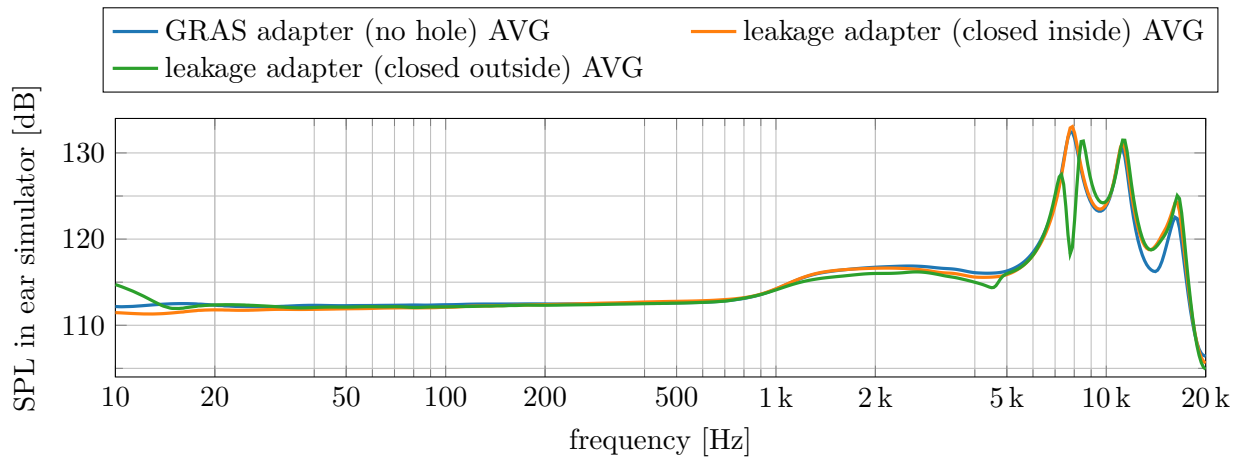
In contrast, a mismatching notch in the measured SPL at 7.9 kHz can be observed when the holes are closed from outside. This notch is caused by the closed $\varnothing 2$ mm venting hole. The closed hole results in a $\lambda/4$ resonator that influences the sound field inside the ear simulator. At its resonance frequency, the wave that is reflected at the closed end of the hole interferes destructively with the incoming wave at the hole's inlet. This explains the observed notch. With the given length of the hole of 10.75 mm, a resonance frequency of $f_{res} = 7.98 \text{ kHz}$ is calculated. This is in very good alignment with the observed notch in the measurement.

The notch at 7.9 kHz was only observed, when the $\varnothing 2$ mm hole was closed from outside. This is the only hole, that has a constant diameter over the full length. All other holes contain a diameter jump after a length of 3 mm (see figure 2.4(b)), which creates reflections. The resonance frequency of these holes therefore is much higher and outside of the studied frequency range.

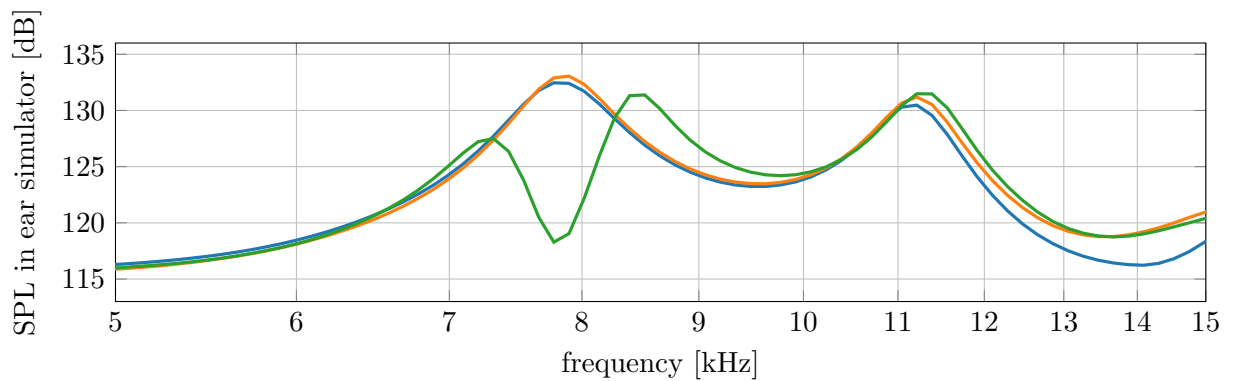
For the investigation of the different venting holes each of the holes has been opened separately, while the others were closed from inside like displayed in figure 3.10(b). Figure 3.12(a) shows a comparison of the four different venting holes with the unvented reference curve, that has been measured with the standard adapter. The high pass filtering effect on the SPL inside the ear simulator is clearly visible, when opening the venting holes. It can be observed, that a larger venting hole leads to a higher cut-off frequency. The cut-off frequency is determined by the Helmholtz resonance of the air mass in the venting hole and the air spring of the enclosed volume. The calculation of the Helmholtz resonance frequency is explained later in this chapter. The resulting resonance frequencies for the different holes are included in figure 3.14.

Figure 3.12(b) shows the simulated results of the same configurations. As described in section 2.3.1, the diameter jump after a length of 3 mm in the $\varnothing 0.2$ mm, $\varnothing 0.5$ mm and $\varnothing 1$ mm holes has been modelled as an open end of the tube. The modelled length of these venting holes therefore is 3 mm, while the $\varnothing 2$ mm hole without diameter jump is modelled with the full length of 10.75 mm.

The same trend as in the measurements can be observed: a larger hole leads to a higher cut-off frequency. For the three larger holes the simulation matches the measurement quite well and the cut-off frequencies are in very good agreement. In contrast, the simulation of the smallest hole ($\varnothing 0.2$ mm) shows a strong mismatch with the measurement. The SPL decreases only slightly at low frequencies and the model shows almost the same behaviour as the model



(a) comparison of the standard adapter with the all closed leakage adapter



(b) zoomed view: relevant notch due to resonance

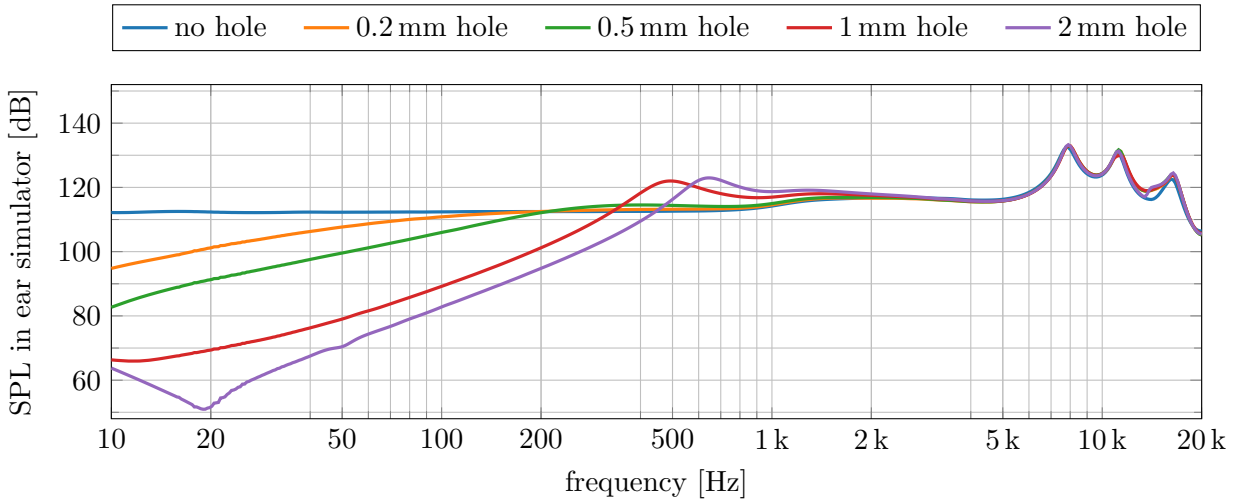
Figure 3.11: closing the holes of the leakage adapter from outside creates a $\lambda/4$ resonator that yields an unwanted notch at 7.9kHz

without any hole. Therefore, it can be concluded that the model's performance is different for different venting sizes. In the following the mismatch for the smallest hole is examined and an empirical adjustment factor is suggested to improve the model's performance for very narrow holes.

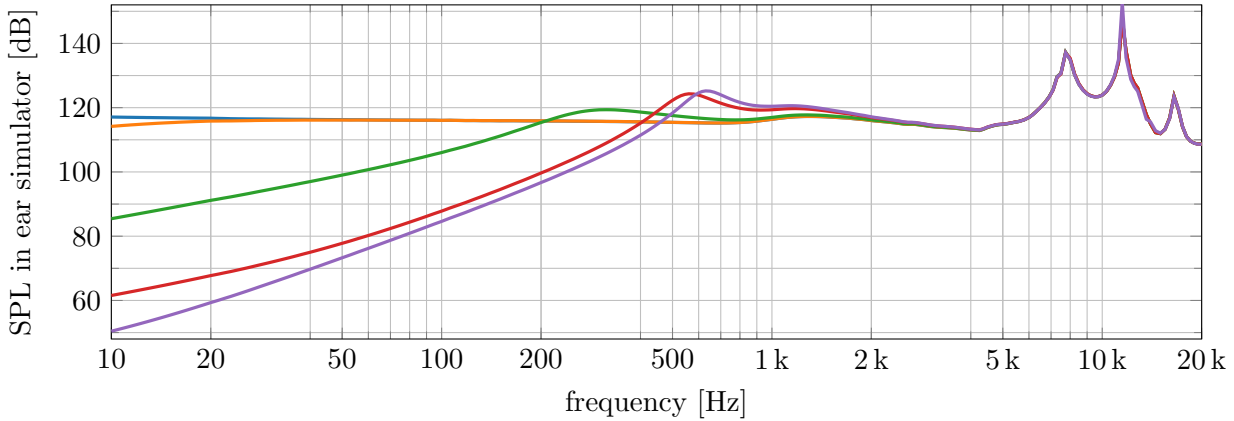
An explanation for the observed behaviour of the model is, that the *Narrow Region* feature in Comsol is modelling the losses inside the venting hole higher than they actually are. The losses are created by thermal and viscous effects in the frequency dependent acoustic boundary layer. When the acoustic boundary layers are overlapping inside the hole, an inaccurate model of the losses becomes most relevant. For the $\varnothing 0.2$ mm hole the overlapping starts already at 500 Hz (see figure 2.6). Therefore, the model of the smallest hole is affected the most by the model's inaccuracy.

As the *Narrow Region* feature does not offer any option to adjust the calculated losses, two different approaches are presented here in order to compensate for the extra losses in the model. First, the length of the venting tube is shortened until the simulation matches the measurement and second, the diameter of the venting tube is increased. Either way will decrease the overall losses in the venting hole and lead to an adjustment factor to improve the model's accuracy.

Figure 3.13(a) shows the results for six different length settings of the $\varnothing 0.2$ mm hole compared



(a) averaged measurements with one hole of the leakage adapter open at a time. The other holes are closed from inside. The reference without holes is measured in the standard adapter.



(b) Comsol simulation with the model described in section 2.3.1

Figure 3.12: comparison of different venting sizes

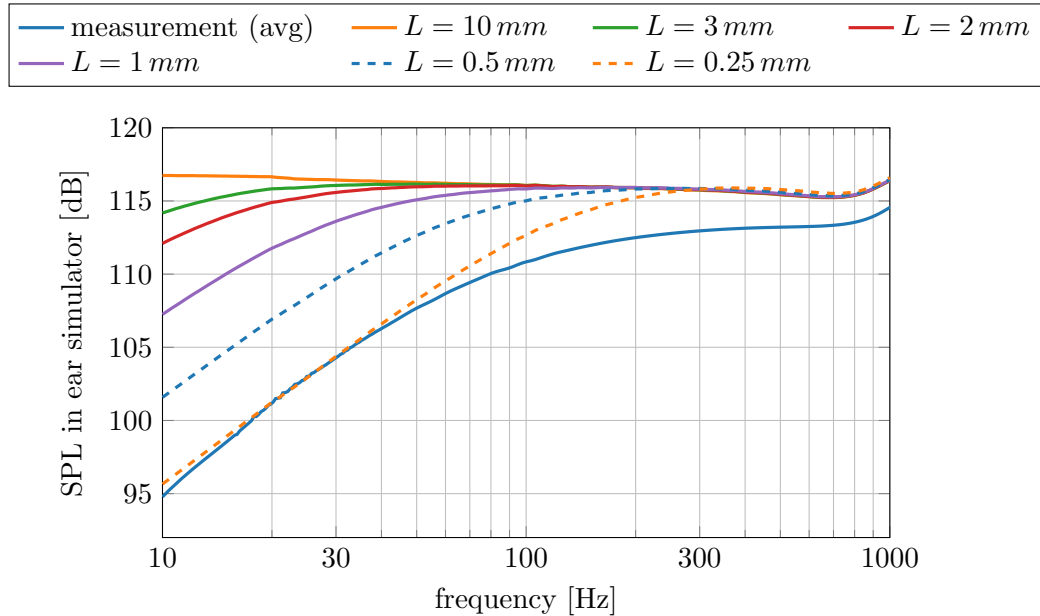
to the measurement. It can be observed, that shortening the venting tube brings back the expected high-pass behaviour. As the change of the length also changes the enclosed acoustic mass inside the venting, not only the damping but also the cut-off frequency is affected by the change. For $L = 0.5\text{ mm}$ the best match with the measurement is achieved. There is still a vertical offset of approximately 5 dB, but the shape of the curve and the location of the cut-off frequency are well matched. Compared to the original length of $L = 3\text{ mm}$ this method results in the following empirical adjustment rule for the simulated length of the venting hole:

$$L_{sim} = \frac{1}{6} \cdot L_{real} \quad (3.1)$$

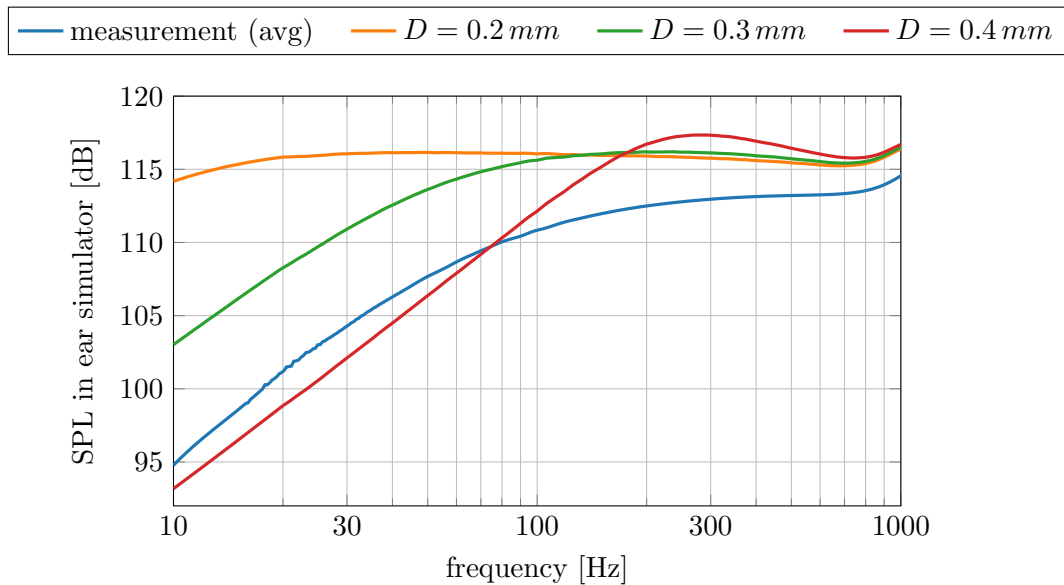
Following the second approach, figure 3.13(b) shows the simulated results for three different diameter settings of the smallest hole compared to the measurement. The length of the venting hole has been kept constant at $L = 3\text{ mm}$. The best fit is reached with a diameter of $D = 0.3\text{ mm}$. Similar to the previous method, a vertical offset can not be avoided, but the shape of the measured curve and the location of the cut-off frequency are reproduced well by the adjusted

model. Compared to the original diameter $D = 0.2 \text{ mm}$ of the smallest hole, this method results in the following empirical adjustment rule for the simulated diameter of the venting hole:

$$D_{sim} = 1.5 \cdot D_{real} \quad (3.2)$$



(a) variation of simulated venting length ($\varnothing 0.2 \text{ mm}$) to adjust simulation to measurement



(b) variation of simulated venting diameter ($L = 3 \text{ mm}$) to adjust simulation to measurement

Figure 3.13: variation of the simulated venting geometry to reduce losses in the smallest hole

Figure 3.14 summarizes the results by comparing the three models with the measurement for each of the studied venting holes. The original model uses the real size of the venting hole as described in section 2.3.1, while the length-adjusted and diameter-adjusted models modify the

modelled venting geometry according to equation 3.1 and 3.2 respectively.

For the smallest hole (see figure 3.14(a)) the adjustment is very important and improves the model's performance significantly. In contrast, for the larger holes (see figure 3.14(b) - 3.14(d)), the real model matches the measurement very well and alternating the model decreases the performance. The unexpected behaviour in the measurement of the $\varnothing 2$ mm hole below 20 Hz should be interpreted as a measurement error due to low frequency vibrations of the measurement setup.

It is therefore recommended to use one of the presented adjustment rules for venting holes with a real diameter of 0.2 mm, and model the venting with its real dimensions for holes with a diameter larger or equal to 0.5 mm. This rule is summarized in table 3.2. For venting holes with a diameter $D < 0.2$ mm or 0.2 mm $< D < 0.5$ mm further investigations are necessary.

real venting diameter	length adjustment ($D_{sim} = D_{real}$)	diameter adjustment ($L_{sim} = L_{real}$)
$D_{real} = 0.2$ mm	$L_{sim} = \frac{1}{6} \cdot L_{real}$	$D_{sim} = 1.5 \cdot D_{real}$
$D_{real} \geq 0.5$ mm	$L_{sim} = L_{real}$	$D_{sim} = D_{real}$

Table 3.2: summary of the empirical adjustment rules for the venting model

In order to understand the observed diameter dependency of the model's performance better, a lossless model has been built, by deactivating the *Narrow Region* feature of the venting tube. The results of the lossless model are also included in figure 3.14. For narrow holes the lossless model is completely off, because the acoustic boundary layers cover a major part of the hole. Neglecting the thermal and viscous losses that appear in the acoustic boundary layer therefore yields a very different behaviour of the model. In contrast, for the biggest hole the lossless model matches the measurement perfectly, because the boundary layer only covers a minor part of the venting hole. Neglecting the losses therefore does not create a relevant change. This explains why an adjustment of the model is only necessary for very narrow venting holes in order to compensate for the increased losses calculated by the *Narrow Region* feature. For wider holes the original geometry of the hole has to be kept in order to not falsify the results.

The shift of the cut-off frequency depending on the size of the venting hole is explained with the model of a Helmholtz resonator. A Helmholtz resonator is an acoustic mass-spring-system. Here, the acoustic mass is the air inside the venting hole and the acoustic spring is the enclosed air volume inside the headphone and the ear simulator. It's resonance frequency is calculated according to equation 3.3 (see [13, p. 61ff.]).

$$f_H = \frac{c}{2\pi} \cdot \sqrt{\frac{S}{l_{eff} \cdot V}} \quad (3.3)$$

Opening Surface S : The circular opening area of the venting hole is calculated as

$$S = r_{venting}^2 \cdot \pi$$

Effective Length l_{eff} : To account for the additional air mass that has to be moved on the inside and on the outside of the venting hole, a radius dependent correction term has to be added to the length of the venting hole.

$$l_{eff} = L_{venting} + 1.7 \cdot r_{venting}$$

Volume of Acoustic Spring V : The air volume inside the headphone, the adapter and the ear simulator works as an acoustic spring. The volume of the resonators inside the ear simulator is included here because their resonance frequency is much higher than the resonance of the venting system. Far below their resonance frequency these mass-spring-systems can be approximated by a simple spring, which is equivalent to an attached air volume. Their volume should therefore be added to the effective volume of the ear simulator here. The total enclosed air volume for $h_{insert} = 5 \text{ mm}$ is:

$$V = 1641 \text{ mm}^3$$

The calculated resonance frequencies for the studied venting holes are listed in table 3.3 and included in figure 3.14 as vertical lines. The Helmholtz model matches perfectly with the lossless simulation.

venting size	Helmholtz resonance
$D = 0.2 \text{ mm}, L = 3 \text{ mm}$	134 Hz
$D = 0.5 \text{ mm}, L = 3 \text{ mm}$	323 Hz
$D = 1 \text{ mm}, L = 3 \text{ mm}$	609 Hz
$D = 2 \text{ mm}, L = 10.75 \text{ mm}$	677 Hz

Table 3.3: calculated Helmholtz resonance frequencies for the different venting holes

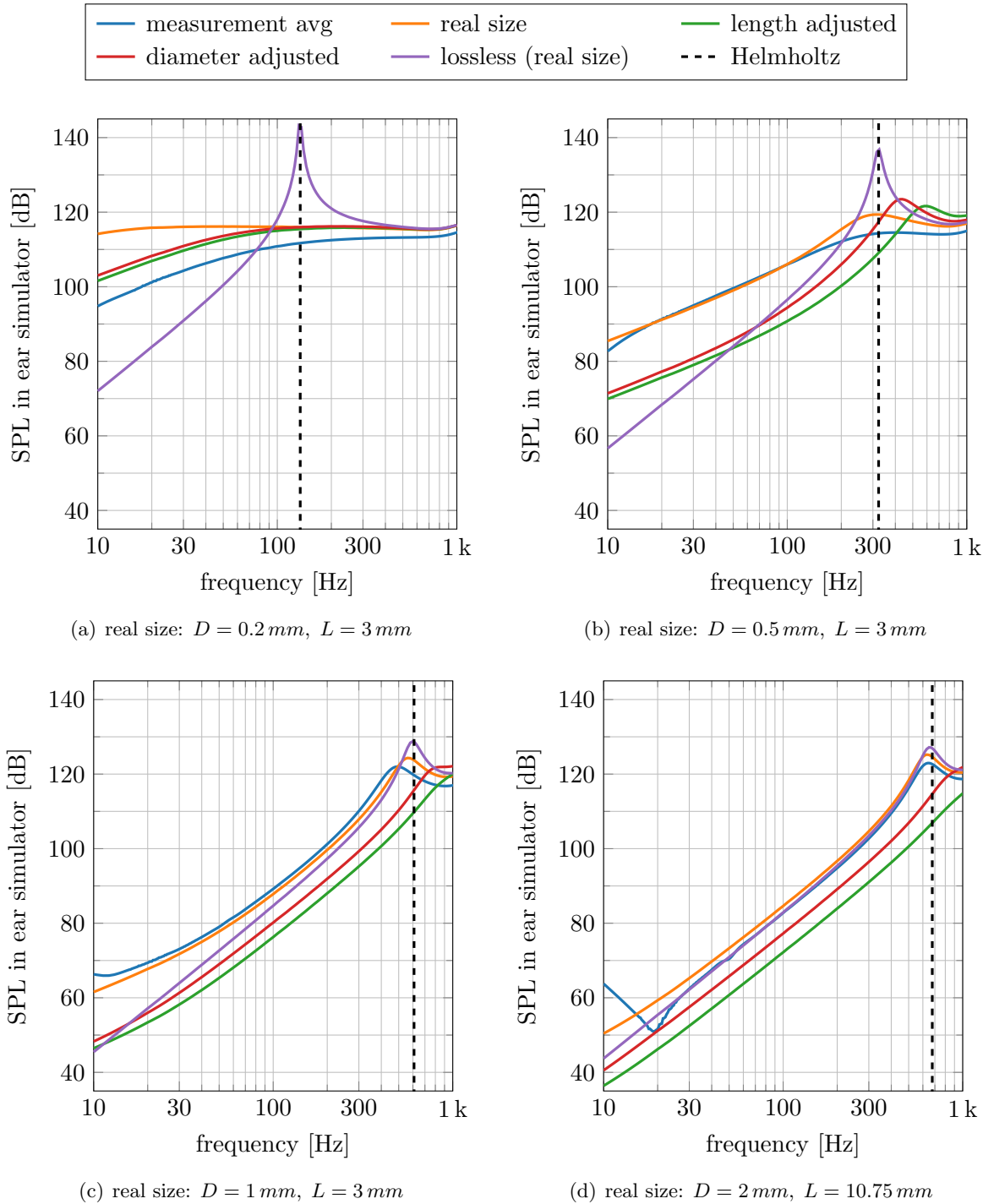


Figure 3.14: comparison of the presented modelling approaches for each of the studied venting holes

3.2.4 variation of acoustic fleece

The outlet of an in-ear headphone is usually covered with an acoustic fleece. This fleece fulfils two purposes: First, it protects the speaker from dirt and mechanical damage and second, its acoustic properties can be used to optimize the headphone's frequency response. Here the fleece is used to damp a resonance, that appears inside the headphone. In order to use the Comsol model for this optimization task, the model of the acoustic fleece has to be validated over the full range of possible fleeces.

Four fleeces of the Saati Acoustex collection with a total airflow resistance $R_{f,tot}$ of $42 \frac{Pa \cdot s}{m}$, $80 \frac{Pa \cdot s}{m}$, $160 \frac{Pa \cdot s}{m}$ and $260 \frac{Pa \cdot s}{m}$ have been chosen to cover the company's typically used range. The fleece has been modelled in Comsol as a poroacoustic domain using the Delany-Bazley model. This is an empirical one-parameter model that only needs the airflow resistivity of the porous material as an input. There are different versions available for the eight coefficients in the model. Three coefficient sets have been shown to be applicable in the desired frequency and airflow resistance range:

- Mechel, glass fibre, low X (abbreviated as glassLoX)
- Mechel, rock fibre, low X (abbreviated as rockLoX)
- Modified Champoux and Allard (abbreviated as Allard)

The Saati Acoustex fleeces, their model and the different coefficient sets are described in section 2.3.2. In this section the three selected coefficient sets are compared to the measurements. The rockLoX model indicates the best performance and is therefore chosen for the headphone model.

The different fleeces have been glued on the outlet of the headphone prototypes (see figure 3.15). The measurements have been done with the standard in-ear adapter without any venting hole and with the reference insertion depth $h_{insert} = 5 \text{ mm}$. The plotted measurement results are the average over the five prototypes.



Figure 3.15: headphone prototype without (left) and with (right) fleece

Figure 3.16 compares the simulated and the measured sound pressure level inside the ear simulator for the different fleeces/airflow resistances. As the fleece does not affect the behaviour at low frequencies, the graphs are shown for the frequency range from 5 kHz to 20 kHz. It can be observed that the three coefficient sets of the Delany-Bazley model yield a very similar behaviour and all of them show relevant deviations from the measurement for frequencies over 10 kHz. As the differences of the three coefficient sets are very small, it can be concluded that further improvements are probably not possible with the Delany-Bazley model. The performance is limited by the fact that this is an empirical model based on only one material parameter - the airflow resistivity. A better approach is to collect more material data about the Saati Acoustex fleeces and then switch to a more-parameter model in the *Poroacoustics* feature.

Nevertheless, the Delany-Bazley model already covers the general behaviour of the different fleeces well, as shown in figure 3.17. Out of the three coefficient sets, the rockLoX model reproduces the strong damping of the second resonance peak best and is therefore chosen to model

the acoustic fleece.

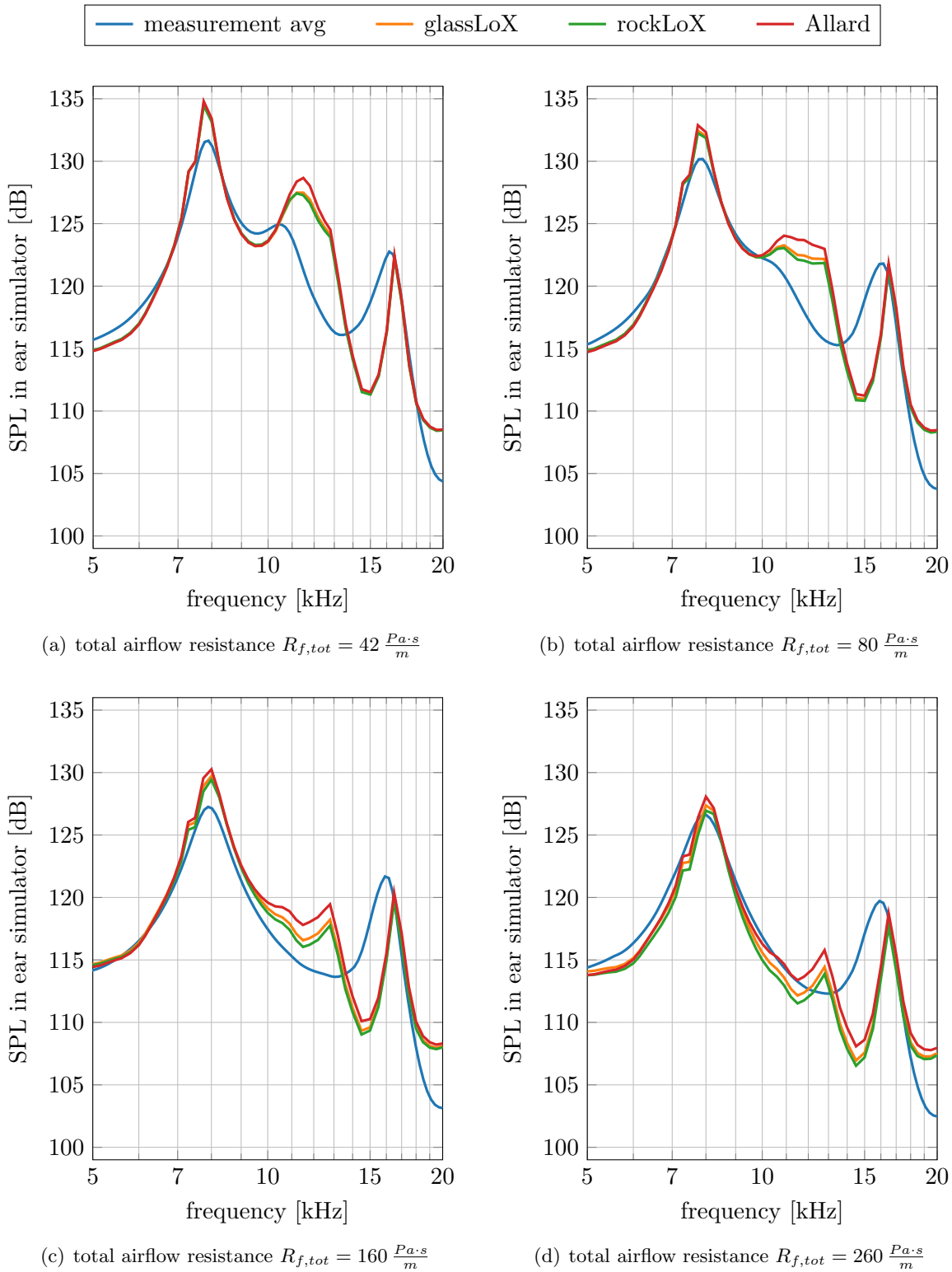


Figure 3.16: comparison of the valid coefficient sets for the Delany-Bazley model in Comsol with the averaged measurement for different acoustic fleeces

To illustrate the effect of the fleece better, figure 3.17 shows a direct comparison of the four different fleeces and the version without any fleece, both for the simulation and the measurement.

It can be observed that the fleece is mostly damping the second resonance peak at approximately 11.5 kHz. A higher airflow resistance of the fleece yields a stronger damping of the peak. This peak is caused by a $\lambda/4$ resonance inside the headphone with a velocity maximum at the fleece. This resonance is therefore strongly damped by the fleece. The first and the third peak at approximately 8 kHz and 16 kHz however, are caused by a $\lambda/2$ and a λ resonance inside the combined air volume of the ear simulator and the adapter, that show a velocity minimum at the fleece. These peaks are therefore only little affected by the fleece. This general trend is reproduced very well by the model. Only the amplitude at the resonances, especially for the undamped case, is too high in the simulation. This can be explained by the fact, that the model is lossless except for the fleece. Therefore, the simulated amplitude at resonance is too high.

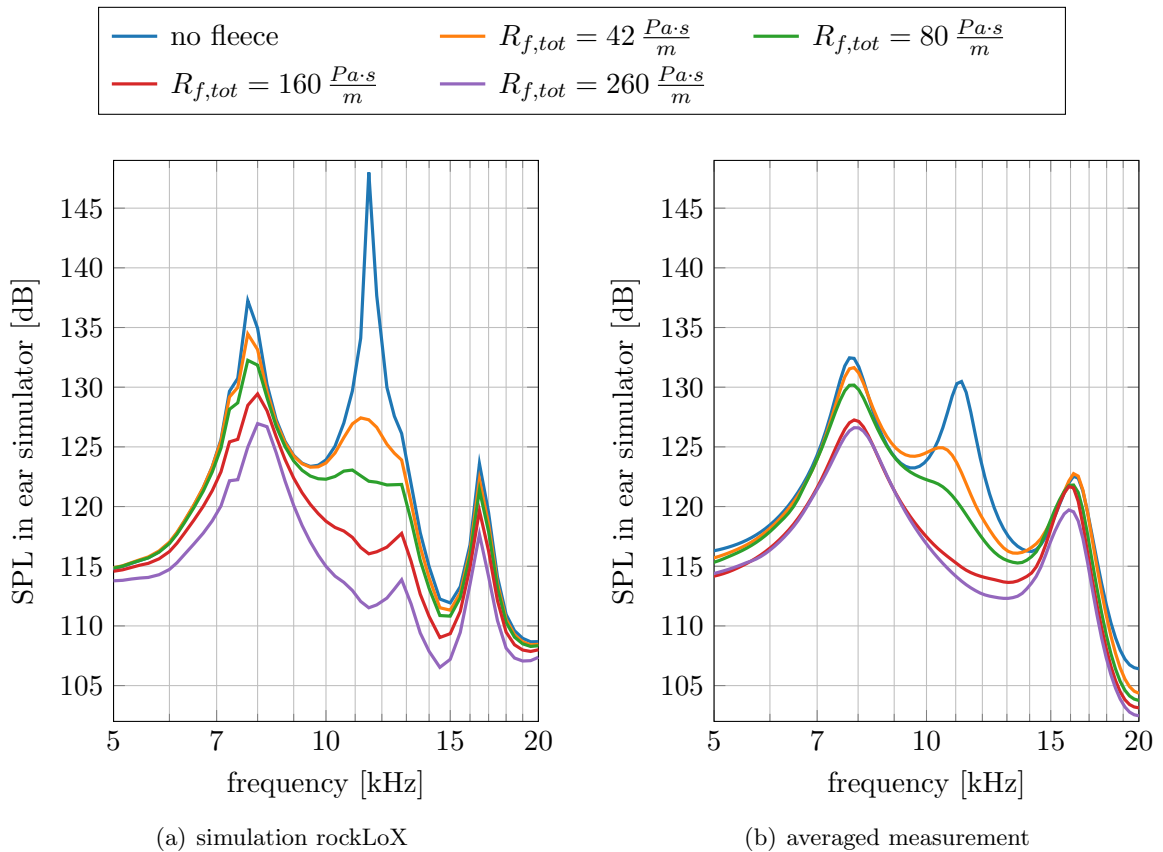


Figure 3.17: comparison of the different acoustic fleeces for simulation and measurement

4

Conclusion

4.1 Summary

In this work, a finite element model of an in-ear headphone in a standardized ear simulator (IEC 60318-4) was developed with the software Cmsol Multiphysics 5.6. The model replicates the typical measurement setup used to evaluate in-ear headphones and serves as the basis for a headphone development application. The model allows easy replacement of the headphones geometry, considers different insertion depths of the headphone and includes submodels for an acoustic fleece and a venting hole.

The wave propagation from the loudspeaker membrane to the microphone in the ear simulator is computed with the *Pressure Acoustics, Frequency Domain* interface. Thus, the Helmholtz equation is solved in the simulation. The venting hole is modelled with the *Narrow Region Acoustics* feature to consider the losses inside the narrow hole. It is terminated with a boundary condition for the radiation impedance of unflanged circular pipes. The acoustic fleece is modelled with the *Poroacoustics* feature, implementing the Delany-Bazley model. Different coefficient sets of the porous model were compared and yielded similar results. The ear simulator is replaced by its input impedance and transfer function, resulting in a perfect match with the full model. Apart from the venting hole and the acoustic fleece, the wave propagation inside the model is lossless.

Measurements of the speaker's membrane velocity were conducted using a laser Doppler vibrometer. The averaged membrane velocity was used as an input to the model by defining a normal velocity boundary condition. Another series of measurements was performed with headphone prototypes in an ear simulator, varying the insertion depth, the acoustic fleece and the venting hole. A special made leakage adapter was used to investigate different venting holes on the same headphone. The measured SPL was used to validate the model.

The simulation largely agrees with the measurement. The shift of resonance frequencies caused by a variation of the insertion depth is represented very well in the model. However, the amplitude at resonance is overestimated because the model is largely lossless. The venting model works very well for diameters greater than or equal to 0.5 mm, but for a \varnothing 0.2 mm hole a correction factor had to be established. The porous model of the acoustic fleece is limited to only one material parameter, but still covers the general damping behaviour of the fleece.

4.2 Limitations and Future Work

The model was created and validated with a specific headphone geometry. However, the headphone development application that will use this model is intended to be used with any headphone geometry. Therefore, it is important to validate the model with different headphone geometries.

The venting hole was modelled using the *Narrow Region Acoustics* feature. This feature was found to give very good results for diameters greater than or equal to 0.5 mm. However, for a hole with a diameter of 0.2 mm, a significant deviation from the measurement was observed. The behaviour of the *Narrow Region Acoustics* feature should therefore be investigated further for very thin venting holes. The established correction factor for the $\varnothing 0.2$ mm hole should be adjusted for other diameters. This requires further measurements with venting holes with diameters of less than 0.5 mm, e.g. using a different leakage adapter with other holes.

The radiation impedance condition that terminates the venting hole assumes that the venting hole opens into free space. In some headphones, however, the venting opens into the back volume behind the speaker instead. A simple model for this case should be developed.

The acoustic fleece was modeled with the *Poroacoustics* feature. For lack of sufficient material parameters, the empirical Delany-Bazley model had to be chosen. It is valid only for highly porous materials. However, the used acoustic fleeces have a low porosity. The results could probably be improved by using one of the more sophisticated porous models. Therefore, the material parameters required for these models should be determined for the used Saati Acoustex fleeces.

The acoustic fleece is modelled in this work at the outlet of the headphone. The model could be extended with other positions for the fleece that can be used in the headphone development application, e.g. at the outlet of the venting hole and in front of the loudspeaker.

The losses in the acoustic boundary layer are largely neglected in the model and are only considered in the venting hole and the acoustic fleece. Consideration of these losses in the entire geometry without limiting its applicability in the headphone development application is not simple. However, it would improve the performance of the model, especially at resonance.

The membrane velocity of the loudspeaker is measured in the free field and used as a fixed boundary condition in the model. To account for a feedback effect of the sound field in the ear simulator on the movement of the membrane, an impedance model of the loudspeaker should be included. This could be further extended by also considering the influence of the back volume behind the loudspeaker.

Bibliography

- [1] USound, “Technical Documentation,” *Achelous UT-P2018 data sheet*, accessed: September 14, 2021. [Online]. Available: <https://www.usound.com/technical-documentation/>
- [2] COMSOL, “Introduction to Comsol Multiphysics,” *Version 5.6*, accessed: September 14, 2021. [Online]. Available: <https://cdn.comsol.com/doc/5.6/IntroductionToCOMSOLMultiphysics.pdf>
- [3] —, “Acoustics Module User’s Guide,” *Version 5.6*, accessed: September 14, 2021. [Online]. Available: <https://doc.comsol.com/5.6/doc/com.comsol.help.aco/AcousticsModuleUsersGuide.pdf>
- [4] —, “Application Gallery,” *Acoustics Module*, accessed: September 14, 2021. [Online]. Available: <https://www.comsol.com/models/acoustics-module?sort=popularity>
- [5] H. Petritsch, “FEM-Simulationen mit COMSOL Multiphysics im Anwendungsbereich der Technischen Akustik,” Master’s thesis, TU Graz, 2010.
- [6] G. Graber and W. Weselak, “Raumakustik Skript V6.1,” SPSC - TU Graz, 2017.
- [7] W. Weselak, “Technische Akustik Skript V15.0,” SPSC - TU Graz, 2019.
- [8] P. Andersen, “Modelling of acoustic viscothermal losses using the boundary element method,” Ph.D. dissertation, Technical University of Denmark, 2018.
- [9] COMSOL, “Theory of Thermoviscous Acoustics: Thermal and Viscous Losses,” accessed: September 14, 2021. [Online]. Available: <https://www.comsol.com/blogs/theory-of-thermoviscous-acoustics-thermal-and-viscous-losses/>
- [10] —, “Open Pipe,” *tutorial model*, accessed: September 14, 2021. [Online]. Available: <https://www.comsol.de/model/open-pipe-1365>
- [11] Saati, “Acoustex data sheet,” accessed: September 14, 2021. [Online]. Available: <https://www.saati.com/sites/default/files/elemento-download/SAATIFIL%20ACOUSTEX%20RANGE.8.pdf>
- [12] COMSOL, “Generic 711 Coupler,” *tutorial model*, accessed: September 14, 2021. [Online]. Available: <https://www.comsol.de/model/generic-711-coupler-8212-an-occluded-ear-canal-simulator-12227>
- [13] G. Graber and W. Weselak, “Elektroakustik Skript V9.0,” SPSC - TU Graz, 2018.